MIXTURE DESIGN TO MITIGATE BRIDGE DECK CRACKING

By

BIJAYA LAXMI RAI

Bachelor of Science in Civil Engineering

Purwanchal University

Biratnagar, Nepal

2013

Submitted to the Faculty of the
Graduate College of the
Oklahoma State University
in partial fulfillment of
the requirements for
the Degree of
MASTER OF SCIENCE
July 2017

MIXTURE DESIGN TO MITIGATE BRIDGE DECK CRACKING

Thesis Approved:

Dr. Tyler Ley

Thesis Adviser

Dr. Julie Hartell

Dr. Xiaoming Yang

TABLE OF CONTENTS

Chapter Page

I. OVERVIEW OF THE THESIS 1

II. REVIEW OF LITERATURE 2

2.1 Introduction and Literature Review 2

III. METHODOLOGY 6

3.1 Experimental Investigation 6
3.1.1 Materials 6
3.1.2 Mix Procedure 7
3.1.3 Mix Procedure 8
3.1.4 Sample Preparations and Casting 9
3.1.5 Curing and Drying Conditions 10
3.1.6 Shrinkage Mass Loss Measurement 12
3.1.7 Calibration of RH sensors: 13
3.1.8 Test Methods 19

IV. FINDINGS AND DISCUSSIONS 20

4.1 Shrinkage Strain and Mass Loss 20
4.2 Mechanical properties 43

V. CONCLUSION AND RCOMMENDATION 58

REFERENCES 59

LIST OF TABLES

Table Page

Table 3.1 The oxide analysis of the cement used in the concrete 8

Table 3.2 The oxide analysis of the fly ash used in the concrete 8

Table 3.3 The mixture proportions used in this experiment(All are in pound) 9

Table 3.4 The results from the slump, unit weight, and air meter tests 10

Table 4.1 showing comparison of all the mixtures 55

Table 4.2 showing comparison of drying day before cracking 59

LIST OF FIGURES

Figure Page

Figure 2.1 Interaction of surfactants with polar molecules (water) [9] 4

Figure 3.2 drying arrangement for all axial beams and curling beams 12

Figure 3.3 Showing measurement of a) axial shrinkage with comparator and b) shrinkage in curling beam 14

Figure 3.4 Compressive strength testing 15

Figure 3.5 Splitting Tensile Test 16

Figure 3.6 Shows Setup for Static Modulus Test 17

Figure 3.7 Arrangement for the Transient Time Measurement 18

Figure 3.8: Electrical resistivity measuring techniques: (a) two-point uniaxial method; and (b) four-point (Wenner probe) method [31] 20

Figure 4.2. The strain change over time for the Type K mixtures. 24

Figure 4.4 Strain change over time for the mixtures investigated as measured by axial comparator. 26

Figure 4.4 (b) Strain change over time for the mixtures investigated as measured by axial comparator for all SRA Samples 28

Figure 5.1 Mass changes over time for the no cure for all mixtures. 30

Figure 5.3 Strain changes at top level of curling beam over time for the no cure for all mixtures. 32

Figure 5.5 Strain changes at bottom level of curling beam over time for the no cure for all mixtures. 34
Figure 5.14: showing typical RH humidity change over time 42
Figure 5.15: showing gradient in RH at different depth for optimized no cure over time 42
Figure 5.16: showing gradient in RH at different depth for optimized 7 days cure over time 43
Figure 5.17: showing gradient in RH at different depth for normal no cure over time 43
Figure 6.1 Compressive strength change over time for the different mixtures. 46
Figure 6.5 Surface resistivity change over time for the different mixtures. 52

CHAPTER I

OVERVIEW OF THE THESIS

The main concern of this study is to develop different mixture designs that help to mitigate bridge deck cracking. The Oklahoma Department of Transportation (ODOT) supported this research project. This study correlates shrinkage measurements with compressive strength, static and dynamic modulus, splitting tensile strength, and resistivity to develop mixture designs with low cracking. Permeability is also one of the factor behind durability and, so, resistivity is investigated in this study.

This study does not consider any autogenous and chemical shrinkage because ODOT prefers water to cementitious material ratio (w/c) in the range of 0.42-0.45 at which these type of shrinkage is not significant. This study does not consider early age tension and compression creep because of budget restrictions.

This study presents several repetition of mixtures and their repeated measurements and test results to investigate repeatability.

Chapter 2 contains only one part 2.1 Introduction and Literature Review, Chapter 3 contains several subsections and Chapter 4 contains two parts: 4.1 Shrinkage Strain and Mass Loss Chapter five talks about Conclusion and Recommendations.

CHAPTER II

REVIEW OF LITERATURE

Cracking in bridge occurs due to various reasons: shrinkage, fatigue, creep etc. Shrinkage is a problem in structures with large surface to volume ratios that are highly restrained such as a bridge deck **[1]**. Shrinkage can be plastic, drying, autogenous or chemical and thermal shrinkage. As most concrete bridge deck designs in Oklahoma have a water to cementitious material ratio (w/c) of about 0.42 -0.45, where autogenous shrinkage is not significant.

Plastic shrinkage occurs due to loss of water from the newly cast concrete. When the rate of evaporation from the concrete surface exceeds the rate of water bleeding that leads to the increase in the capillary pressure near the surface **[2]**. This is typically attributed by the high temperature, high wind, low ambient relative humidity, mixture ingredients and proportions **[3]**. Drying shrinkage occurs due to continued moisture loss from the surface of the concrete due to capillary action until the internal RH humidity of the concrete becomes equal to the outside environment.

Rubin, 2006, states that most bridge constructed with concrete has cracks. Cracks allow ingress of salts causing corrosion in the reinforcing steel, and other durability problems. When concrete dries it shrinks, it produces tensile stresses in the concrete. The reinforcing steel restrains this shrinkage. Hence, it produces compressive stresses in the rebar.

Concrete is composed of two different phases: cement paste and aggregate. Volumetric changes occur in cement paste while aggregate is volumetrically stable and provides internal restraint to the shrinkage of the concrete. Only certain aggregates are porous and may experience the

shrinkage in small amount but it is very less in comparison with paste. The cement paste shrinks when the moisture content is lost due to surface tension of water and menisci formed in pore spaces in the paste. The amount of paste shrinkage depends upon volume of cement paste, w/cm, cement type, cement fineness, stiffness of aggregate, anything that affect pore size distribution, and the bond between the paste and the aggregate affect the shrinkage in concrete.

This study used two different types of mix designs: normal mix design-which has only one coarse aggregate (#57) and fine aggregate and other, and an optimized graded mix design, which has two different coarse aggregates (#57 and 3/8) and one fine aggregate.

Mindess and Young, 1981, suggested that the use of stiffer aggregate and low volume of cement paste can reduce the shrinkage in the concrete **[4]**. Further, they state that concrete mixtures made using higher cement contents are likely to produce cracks by producing higher heat of hydration, greater shrinkage, higher modulus of elasticity. Use of optimized concrete mixture has the potential to help with these issues. Our study used shrinkage reducing admixtures (SRA), expansive cement (Type K cement), and pre-saturated fine light weight aggregate (SLA) to further reduce the propensity for cracking.

As the name says, SRA is used for reducing the shrinkage in concrete. The addition of SRA to the control concrete mix yields a shrinkage reduction of 35% at 28 days and 29% at 120 days. The combination of silica fume with SRA showed much higher percentage of reduction in shrinkage than silica fume alone **[5]**, while,**[6]** states that SRA can reduces shrinkage up to 80% in 28 days. In this study, 10% of SRA is used as the replacement of water. SRA reduces the surface tension of pore fluid when added up to a threshold concentration up to 7.5%. Above this critical threshold, further addition of SRA results in further reduction in pore fluid's surface tension becomes marginal **[7]**.

SRA is amphiphilic surfactants – hydrophilic head (attracted to water) and hydrophobic tail (attracted to non-polar solvent like oil). Adsorption of surfactants reduces the water-air interface – i.e. reduces surface tension **[8, 9]**. However, this happens only when the addition of surfactants is below critical micelle concentration (CMC). Above this, excess surfactant molecules form micelles in the bulk of water and cannot serve further to reduce surface tension **[8]**. The figure below illustrates the mechanism:

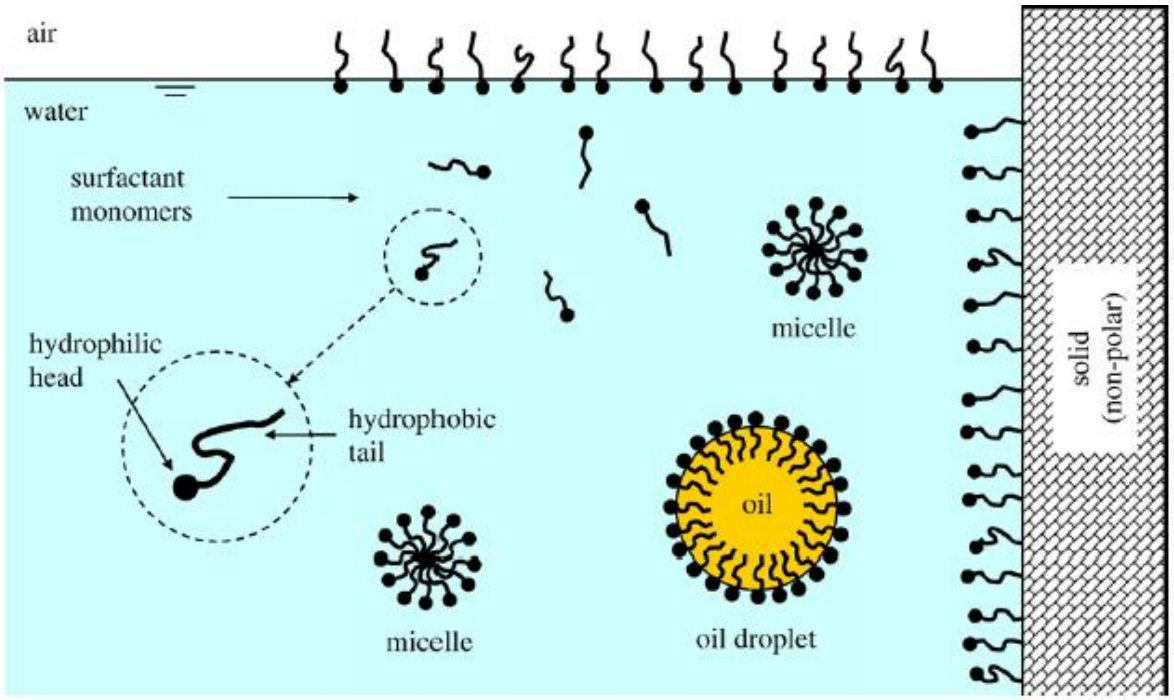

Figure 2.1 Interaction of surfactants with polar molecules (water) [9]

SRA reduces the rate of cement hydration and the strength development **[7]**. It is because SRA gets dissolved in mixing water, remains in the pore system of concrete and reduces the surface tension of water **[6]**.The strength reduction is as high as 25% for 1 day, however, the rate is reduced to around 10 % for 28 day concrete **[5]**. Others have reported that when SRA is used at 2% by weight of cement of dosage level, results reduction in compressive strength approximately by 10% at 28 days. **[6]** States that compressive strength can go down by up to 15% but it also

depends on the w/c ratio and the dosage of SRA used in the concrete mix. Nevertheless, there is no significant difference in the rapid chloride permeability test, which indicates that it might not have impact on resistivity of concrete.

The use of expansive cement attempts to offset the effect of shrinkage and has been used in several bridge projects**[10]**. When concrete shrinks, it produces tensile stresses, when these stresses exceed the tensile strength of the concrete, then concrete will crack**[11]**, however, concrete with Type K cement swells as it hydrates and offsets the later age shrinkage.

Gruner and Plain **[12]** noted that the Type K cement as specified by ASTM C 845 has sulphoaluminate, which during hydration produces calcium aluminate, which is commonly known as ettringite, an expansive material.

Many DOTs are using internal curing in bridge decks, such as Illinois, New York, Utah and many more states are experimenting its use **[13]**. The use of lightweight aggregate was thought to reduce weight and modulus of elasticity**[14]**. Nevertheless, later they found that due to inherent property of LWA, as internal curing, provides water for increased hydration that results in a denser microstructure and increased strength due to rough texture increases the bond strength. Two publications have suggested reduced residual stress and stress concentration around the aggregate due to enhanced strain compatibility with cementitious matrix which actually reduce the cracking **[2]** and **[14]**.

However, Shin **[15]** et al investigated the mechanical properties and found out that there is slight decrease in splitting tensile strength (ASTM C 496), modulus of elasticity (ASTM C 469-02) and compressive strength (ASTM C 39). The decrease in mechanical property is inversely proportional the volume of LWA. Field experience showed similar workability, strength, other mechanical properties as well as reduced stress development and improved durability especially cracking as compared to conventional concrete**[13]**.

Shin **[15]** et al also found another positive impact of LWA i.e reduction in ASR as LWA provides free space for expansive gel and also it dilutes and changes the pore solution composition.

CHAPTER III

METHODOLOGY

3.1 Experimental Investigation:

3.1.1 Materials:

The mixture proportion used is presented in Table 2.3 for a cubic yard. The non-optimized mixtures had a w/cm of 0.45 and a total cementitous content of 6.5 sacks (611 lbs) which is typical for bridge decks in Oklahoma. The optimized mixtures had the same w/cm with a total cementitious content of 6 sacks (564 lbs). Two mix designs- sack 6 - one with two different coarse aggregates (#57 and 3/8) and fine aggregate and sack 6.5 with two different coarse aggregates (#57 and 3/8) and fine aggregate were adopted for this research. All the batches used commercially available ASTM type 1 Portland cement, natural sand as fine aggregate, coarse aggregate confirming ASTM C-33 (2016) **[16]**. The coarse aggregates were washed to remove dirt to get better bonding with paste in the concrete. Depending upon the different mix designs, Shrinkage reducing admixtures (SRA), and Saturated Light weight Sand (SLS) and expansive cement-Type K as per ASTM C845 **[17]** were used.

The cement used for concrete samples is type I, according to ASTM C150 **[18]**, and its chemical analysis is shown in the Table 3.1. Samples were made with dolomitic limestone aggregate and natural river sand used commercially in concrete.

Table 3.1 The oxide analysis of the cement used in the concrete

Chemical test results (%)					
SiO_2	Al_2O_3	MgO	Fe_2O_3	CaO	SO_3
20.77	4.57	2.37	2.62	62.27	3.18
Na_2O	K_2O	TiO_2	P_2O_5	SrO	BaO
0.19	0.32	0.34	0.14	0.22	0.07
Phase concentrations (%)					
C_3S	C_2S	C_3A	C_4AF		
52.13	20.22	7.68	7.97		

An ASTM C618 **[19]** class C fly ash with chemical analysis shown in Table 2.2 was also used.

Table 3.2 The oxide analysis of the fly ash used in the concrete

Chemical test results (%)						
K_2O	BaO	MgO	SrO	CaO	SO_3	Na_2O
0.58	0.72	5.55	0.39	23.12	1.27	1.78
SiO_2	Al_2O_3	MnO_2	P_2O_5	Fe_2O_3	TiO_2	
38.71	18.82	0.02	1.46	5.88	1.35	

3.2 Mix Proportions:

For mixtures with SRA, 10% of the water was replaced with the SRA. For mixtures with the Type K cement, the Type K additive and the fly ash was used at a 20% replacement rate by mass

of the cement. For SLA mixture, LWA based on its absorption, desorption and specific gravity, 54.18% volume of sand is replaced with fine light weight aggregate as specified by Weiss 2015, **[13]**.

Table 3.3 The mixture proportions used in this experiment(All are in pound)

Material	Control		SRA		Type K		SLA	
	6.5 Sack	6 Sack	6.5 Sack	6 Sack	6.5 Sack	6 Sack	6.5 Sack	6 Sack
Cement	489	451	489	451	367	338	489	451
Flyash	122	113	122	113	122	113	122	113
57 Stone	1835	1412	1835	1412	1835	1412	1835	1412
3/8		453		453		453		453
Sand	1195	1335	1195	1335	1195	1335	720	806
Water	275	254	248	229	275	254	275	254
Additives			27	25	122	113	269	301
			SRA		Type K		SLA	

3.3 Mix Procedure:

All the aggregate, both coarse and fine, were brought into the temperature controlled mixing facility at least a day before and their batch weights were corrected based on the moisture content of the aggregates. The aggregates were charged into the mixer along with approximately two-thirds of the mixing water. The combination was mixed for three minutes. Next, any clumped fine aggregate was removed from the walls of the mixer. Then the cement and fly ash is loaded into the mixer, followed by the remaining mixing water. The mixer was rotated for three minutes. Once this mixing period was complete, the mixture was left to “rest” for the following two minutes while the buildup of material along the walls was removed. Next, the mixer was allowed to run for three minutes and the water reducer was added as well.

For the SRA mix, SRA was charged and rinsed the bucket with remaining one third of water.

For the Type K mix, the Type K cement was charged with Ordinary Portland cement and fly ash.

For the SLA mix, the fine light weight aggregate was soaked in water for 48 hours and allowed to drain water for 12 hours before the concrete is batched.

The slump (ASTM C143) **[20]**, unit weight (ASTM C138) **[21]** and the air content (ASTM C231) **[22]** were measured. The results are presented in Table 3.4.

Table 3.4 The results from the slump, unit weight, and air meter tests

Mix	Slump (inch)	Unit weight (lb/ft^3)	Air (%)
6 Sack Control	3.75	150.56	
6 Sack Control-I	3.5	151.12	2.5
6 Sack Control-II	5	150.48	
6.5 Sack Control	6	153.2	0.8
6.5 Sack Control-I	6.25	154.88	0.9
6 Sack SRA	4	150.4	3.1
6.5 Sack SRA	7	150.44	2
6 Sack Type K	3	150.56	3
6 Sack Type K-I	1.5	150.4	3
6.5 Sack Type K	3	152.16	1.8
6 Sack SLA	5	144.72	
6.5 Sack SLA	5.5	144.18	0.8

Few mixes do not have air data. This is because air meter was not functioning that day.

3.1.4 Sample Preparations and Casting:

Four beam samples were prepared for linear shrinkage (ASTM C 157) **[23]**. Two of these samples were used for weight loss and axial length change and two of these samples contained vibrating wire strain gauges (VBWG) and these were used to measure the axial strain. These strain gauges were placed in the beams before the concrete was cast and they allow immidiate strain measurements to be made on setting. This allows even the very early strains of the concrete to be measured as it is hydrating. One common criticism of ASTM C 157 is that this technique can not measure these early strains. The usage of the VBWG will help overcome this. After demolding an initial weight was taken and then the samples were placed in a room at 50% RH and 73^{o}F.

Six 10”x4”x3” curling beams were prepared as per the description in literature **[24]**. Out of six, three did not receive any curing and other remaining three were cured for 7 days. In all of these six curling beams were cast in burlene. In each type, one of the sample is provided with holes at three different levels (0.5” below top surface), middle (at middle of beam) and at the bottom (0.5” above the bottom), in order to measure internal relative humidty with the help of I-buttons, which can be correlated to the mass loss and shrinkage. Similary, demac points are inserted in three different heights of the sample to measure the shrinkage at the same levels as the RH gauges. Since the sample can lose moisture only from the top, this causes a moisture gradient. This leads to differential shrinkage in the sample, which ultimately leads to curling of the beam. This is the reason why it is termed as curling beam.

In addition, 4”x8” concrete cylinders were made for compressive strength testing (ASTM C39), static modulus (ASTM C 469), dynamic modulus (ASTM C 215) **[25]**, splitting tension (ASTM C 496), and resistivity (AASHTO TP95)**[26]**.

3.1.5 Curing and Drying Conditions:

All axial shrinkage beams were cured for 7 days in a temperature and humidity controlled room: temperature at 73ºF and relative humidity at 100 %. Axial beam after 7 days of wet curing were kept in the drying room. The drying room temperature was always maintained at 73ºF and relative humidity at 50 %.

There are two types of curling beams: one cured for 7 days with wet burlap and another which never received any curing. Both of them were kept into the drying room.

The cylinders were always cured in temperature and humidity controlled room: temperature at 73ºF and relative humidity at 100 percentage. These cylinders are picked directly from the controlled room and tested on third, seventh, twenty eighth and fifty sixth day.

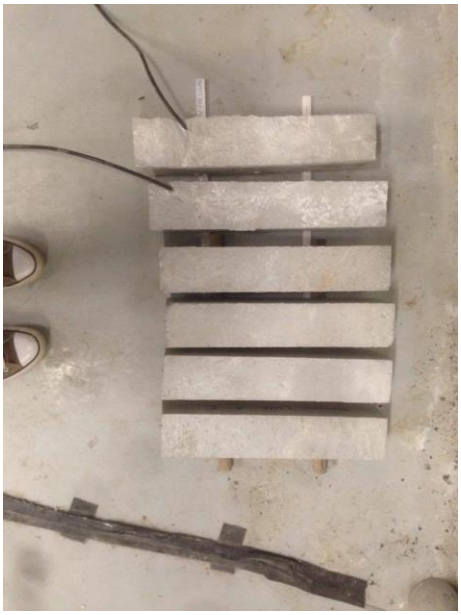

Figure 3.2 drying arrangement for all axial beams and curling beams

3.1.6 Shrinkage Mass Loss Measurement

The mass loss is measured with the accuracy of 0.1g (0.00022lb). The concrete losses the moisture until the internal relative humidity of concrete becomes similar to the environment.

The ASTM C 157 was demolded after a day and the length weight change was measured over time. The concrete prisms with the VBWG was also demolded after a day but the measurments were constantly being made. There were a few gaps in the VBWG measurements. These gaps were because the datalogger had to be unhooked so that other samples could be measured while casting. This was only for a few days. The change was practically constant for these samples at this point and so this should not impact the measurement results.

The results from the testing have been averaged and error bars showing one standard deviaiton have been included.

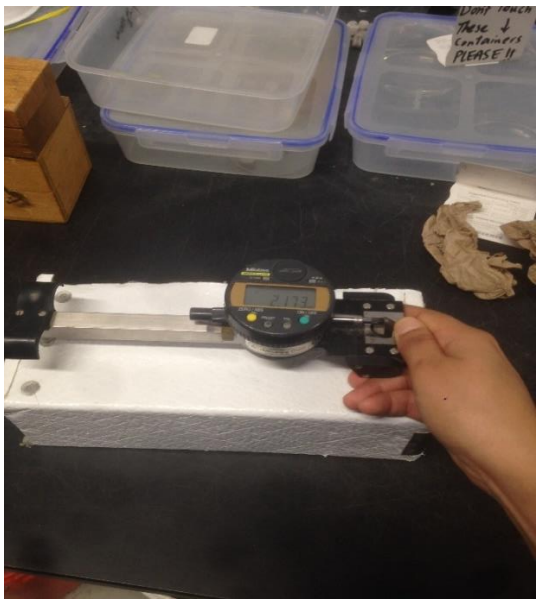

Figure 3.3 Showing measurement of a) axial shrinkage with comparator and b) shrinkage in curling beam

3.1.7 Calibration of RH sensors:

The iButton sensors were calibrated according to ASTM E 104 "Standard Practice for Maintaining Constant Relative Humidity by Means of Aqueous Solutions" with four different salt saturated solutions. The relative humidity calibration range was between 30% to 100% in order to cover the ranges of humidity expected while testing. A specific calibration was generated for each iButton.

3.1.8 Test Methods

3.1.8.1 Destructive Test Methods:

Compressive Strength*:* Three concrete cylinders from each mix were tested for compressive strength at 3, 7, 28 and 56 days as per ASTM C39/39M **[27]**. First, the cylinder were brought nearby the testing machine, removed any surface water with towel and made saturated surface dry (SSD). Then, two bearing metal plates with neoprene pad were kept on top and bottom of the cylinder and placed inside the test machine. The load is applied at the rate of 35±7 psi/s. When the concrete is subjected to uniaxial compressive loading, cracks tend to develop parallel to the maximum compressive stress. However, there will be friction between the testing machine and ends of the cylinder that prevents lateral expansion at the ends and vertical cracking too; so, concrete fails around midheight where lateral expansion is possible. The cylinder breaks in some unique shapes as described in the ASTM standard. When the cylinder breaks, the machine stops and shows peak stress and peak load. The peak stress and peak load are recorded for three samples. Usually, when a measurement showed a significant variation then the test was repeated.

Figure 3.4 Compressive strength testing

Splitting Tension: The splitting tensile strength is obtained by testing three cylinders as per ASTM C 496 **[28]**. Here, diametric compressive force is applied perpendicular to the longitudinal axis of the cylinder so that it produces tensile stresses as the load spreads in the body. The sample is kept over wooden bearing and the metal platen on the both sides and the load is applied. At the end, the sample splits into equally two parts horizontally as shown in the figure below.

Before the test setup, dimensions of samples were measured; length was measured in diametrically opposite side and diameter was measured near two edges and one middle using Vernier caliper. Once the sample broke, ultimate load was recorded. The magnitude of applied tensile stress is given by formula:

$$\sigma_t = \frac{2*P}{2*\pi*r*l}$$

Where P = Ultimate load, r = radius of cylinder, l = length of cylinder

Three samples were tested and found out the average and standard deviation for each test. The standard deviation for this test should not exceed more than 11%, quite larger than in other destructive test.

Figure 3.5 Splitting Tensile Test

Static Modulus: As in other above, three cylinders are tested for the Static Modulus as per ASTM C 469 **[29]**. First, moisture is removed from the surface of the cylinder and measure length and diameter of the each sample. The length is measured in exactly in diametrically opposite and diameter is measured in three places: top, middle and the bottom. Afterwards, the cylinder is placed in a special case which holds the cylinder in three places: top, middle and the bottom. When the load applied on the sample, it assumes that concrete contracts and expands in transverse. About 40% of load is applied for three times assuming that up to this amount of load. The load displacement response remains approximately linear at the range of 40-50% of ultimate load and afterwards stress-strain result diminishes due to the growth of micro cracking in the specimen by which decreases the elastic modulus**[30]**.

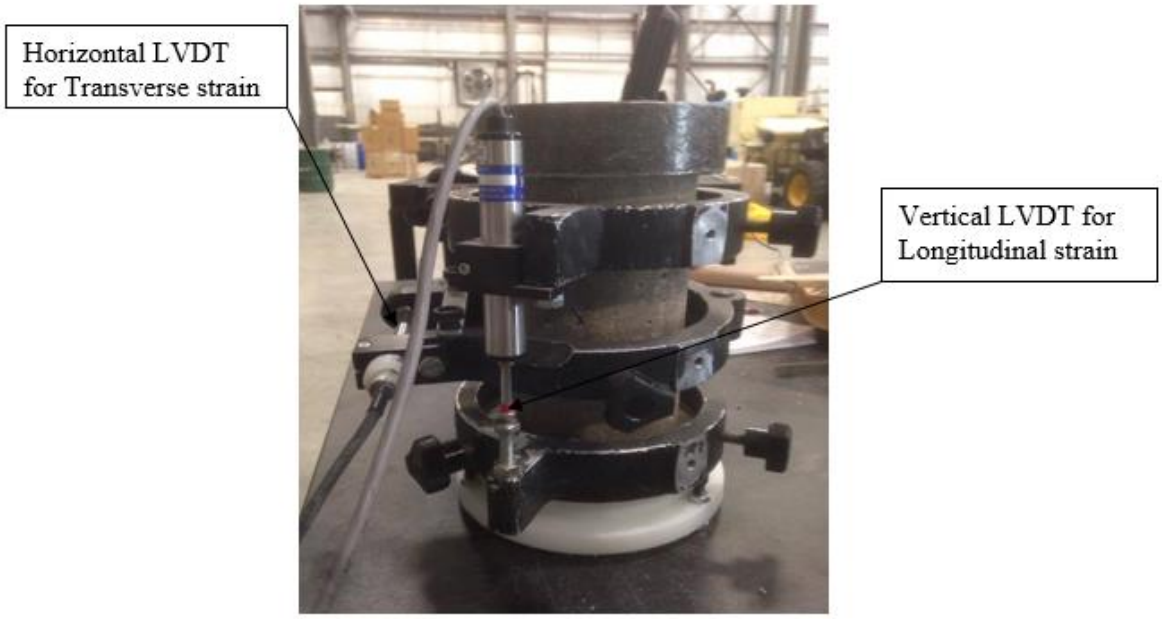

Figure 3.6 Shows Setup for Static Modulus Test

The Modulus of Elasticity is given by:

$E = (S_2 - S_1) / (\epsilon_2 - 0.00005)$

Where:

E = chord modulus of elasticity, psi,

S_2 = stress corresponding to 40 % of ultimate load,

S_1 = stress corresponding to a longitudinal strain, ϵ_1 of 50 millionths, psi, and

ϵ_2 = longitudinal strain produced by stress *S2*

3.1.8.2 Non-Destructive Test Methods*:*

Dynamic Modulus Test:

Standard test for pulse velocity and shear velocity:

Grinded concrete sample is supported in a rigid support and the transducer with the help of coupling agent, viscous material, usually petroleum gel is used to transfer energy from transducer to concrete. A pulse is generated. This triggering pulse initiates the time measuring circuit. The transit time will then displayed in the screen. Display unit measures time up to the accuracy up to 0.1 microsecond.

A 54 KHz transducer is used for pulse velocity and 250 KHz for shear velocity. For shear wave, transducer is rotated and output is displayed in the computer screen.

Accuracy varies with degree of saturation, Relative humidity and coupling agent too.

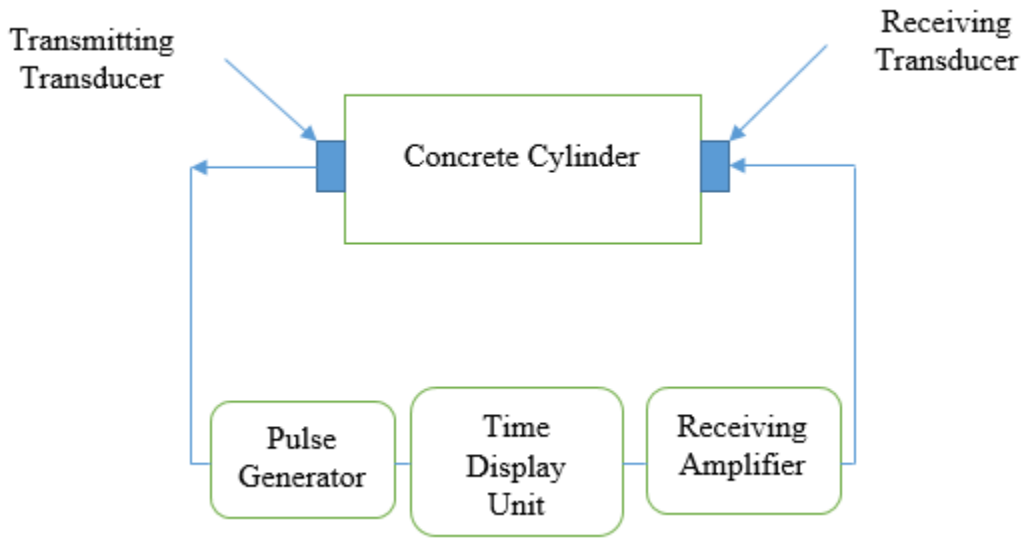

Figure 3.7 Arrangement for the Transient Time Measurement

Poisson's ratio (υ) = $((V_p^2)/2 - V_s^2)/ (V_p^2 - V_s^2)$

Dynamic Modulus of Elasticity (E_d) = $2V_s^2 * \rho * (1+\upsilon)$

Where V_p = Velocity of Compression wave

V_s = Velocity of Shear wave

ρ = density of the Concrete sample

Resistivity Test:

As per AASHTO TP 95 **[26]**, two different resistivity tests: bulk and surface resistivity tests were used in this research. The electric resistivity of concrete is affected by various factors such as pore size distribution, their connections, degree of saturation, conductivity of pore fluid, temperature, pore solution chemistry, contact properties of the electrode and signal frequency. If the internal pores are well connected and saturated then concrete will have less resistivity. Therefore, it is always important to keep the concrete samples saturated surface dry and need to do test in the room with constant temperature and Relative humidity to maintain consistency of the test.

Bulk Resistivity: Bulk Resistivity is measured using two point uniaxial method. Here, test samples are kept standing position as shown in figure below. The two steel plates are electrodes with wet sponge is placed on the both sides of the specimen. The AC was applied and measured the drop in potential. The upper steel plate is pressed against the specimen with arms in order to make sure proper electrical conductivity of the electrodes. These two plate electrodes were connected to the battery. First generates current in the concrete and then measures potential difference between these two electrodes.

The resistance of sponges is largely depends on moisture content, so, we need to provide large pressure from top by putting both hands on it.

Surface Resistivity: The surface resistivity is measured using four point Wenner probe method. First, four lines are marked on Surface saturated dry (SSD) concrete samples in circular cross-section at 0, 90, 180, 270 degree. Afterwards, these lines are equally divided into four marks. The

samples are kept on rigid support and with the Wenner probe, surface resistivity is measured rotating four times. The test is performed in room temperature and ordinary relative humidity. Out of four probes, two probes measure potential difference due to the current flowing in the concrete and the current is applied on the two outer probes.

In this study, I used Resipod Proceq, which directly gives value of resistivity in K-ohm-cm, so no need to do further calculation.

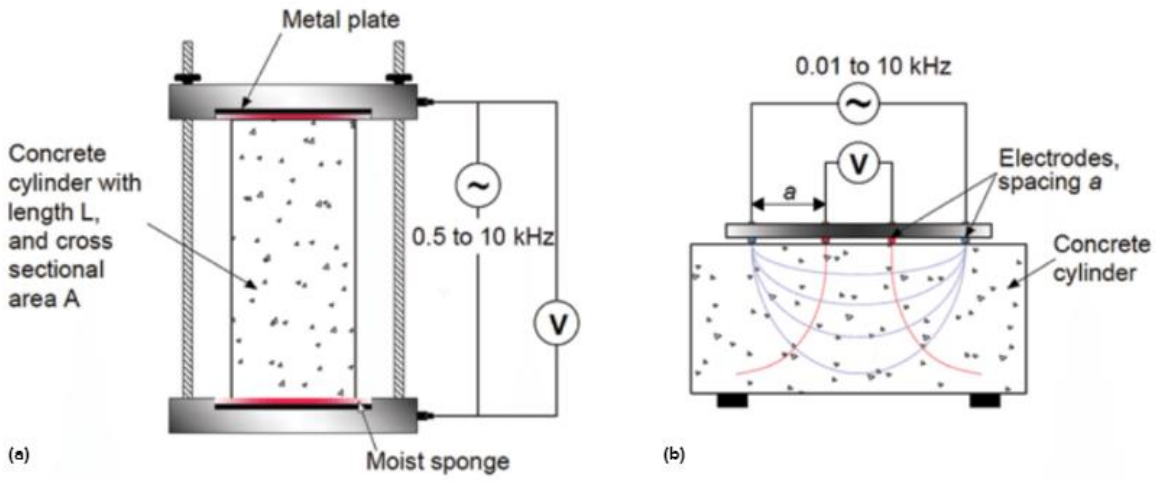

Figure 3.8: Electrical resistivity measuring techniques: (a) two-point uniaxial method; and (b) four-point (Wenner probe) method [31]

CHAPTER IV

FINDINGS AND DISCUSSIONS

4.1 Test Results and Discussions:

4.1.1 Shrinkage Strain and Mass Loss

The shrinkage strain change over time as measured by the VBWG is shown in Fig. 4.1 and the results with the comparator are shown in Fig. 4.3. The VBWG measures shrinkage right from the beginning of placing the concrete in the molds, thus it includes all the thermal shrinkage that occurs during hydration that occurs between 12-18 hours after casting. The comparator shows similar shrinkage but it excludes initial 24 hours shrinkage values. Nevertheless, these two measurements go hand to hand and supports the results.

The results show that the samples swelled over the first 7 d and then started to shrink when the samples were placed in the 50% RH and 73^{o}F room. The average and standard deviation are shown for each of the mixtures. The closer the value is to zero the better the performance is in the test. For all of the mixtures the reduced paste content showed an improvement in shrinkage performance. The SRA seems to be performing the best of the shrinkage reducing technologies. The Type K data is quite variable. In fact, one of the samples is not included in Fig. 4.1 or Fig. 4.3 because of the variability of the measurement. All of the Type K measurements are included in Fig. 4.2 and Fig. 4.4. as can be seen from this figure the results are quite variable. This makes

this technology very hard to adopt because of the wide variation in performance. This high variability has been reported in the literature by others and seems to be inherent of the materials. This is an area of future research.

The SRA showed outstanding performance and looks very promising. While there was very little difference in the shrinkage between the two samples, it is still recommended to use the mixture the 6 sack content as it will have a reduced cost because of reductions of cement content and SRA content over the other mixtures. It is anticipated that the air content testing will need to be modified. This is currently being investigated.

Axial Shrinkage and Mass Loss:

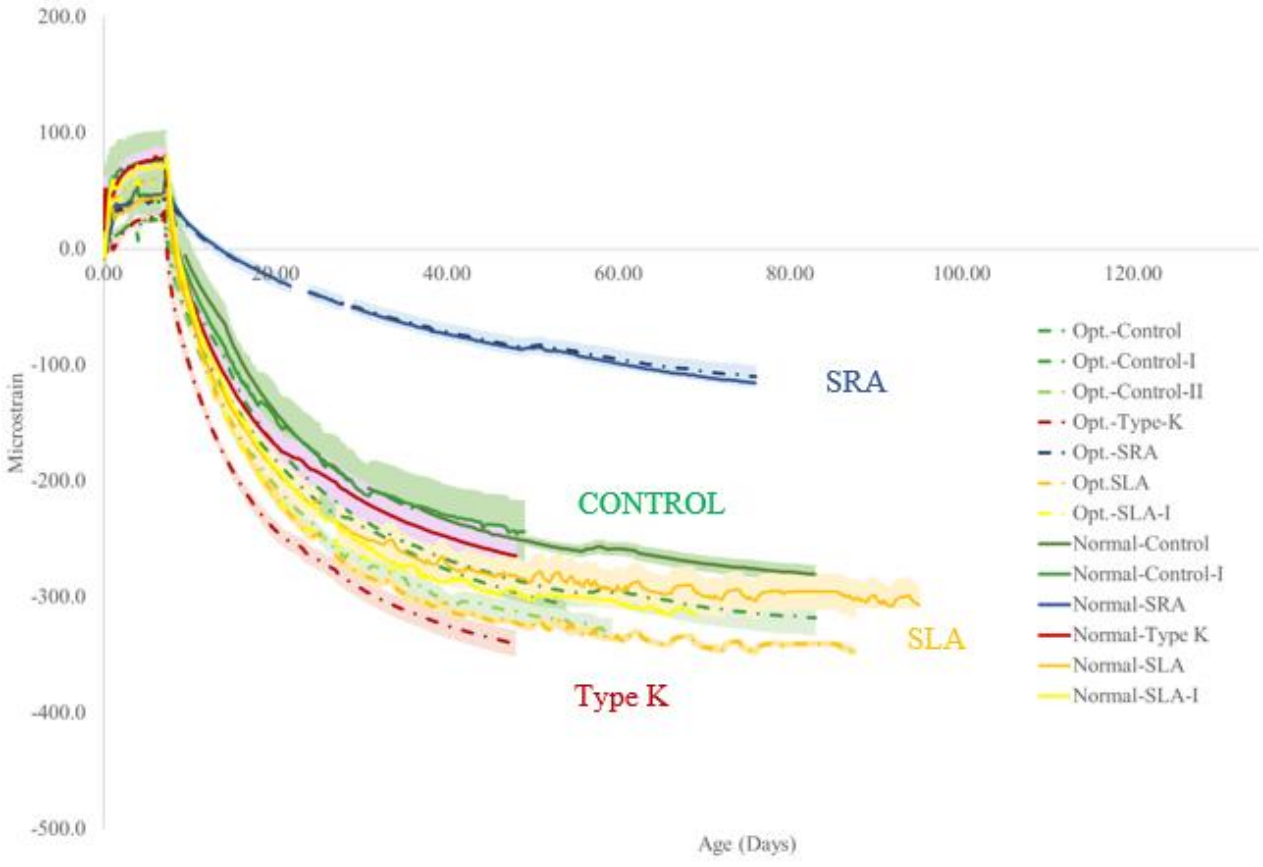

Figure 4.1 Strain change over time for the mixtures investigated as measured by VBWG. Note:

One Type K mixture is not shown. All Type K mixtures are shown in Figure 4.2. (Solid line for Normal and dotted line for optimized.

Usually, the mix design, which has more paste, normal mix in our case, is expected to have more shrinkage since shrinkage is directly proportional to the paste volume. In reverse, shrinkage is inversely proportional to the aggregate volume due to its restraining properties.

The SRA sample is showing about 80% reduction in shrinkage as compared to control samples which supports the findings from previous literatures, **[5, 6]**.This is positive result for us. It might be due to better mix design, w/c ratio, aggregate volume etc.

Even with light weight aggregate, Browning,**[32]** found out shrinkage more than 350 micro strain in 30 days and claimed that to be reduced shrinkage as compared to his control mix without light weight aggregate. In our case, we are getting less than 300 micro strain shrinkage in 30 days and even less than 350 micro strain shrinkage at the last day of measurement as in figure 3.1. The difference might be due to the use of different type and different amount of lightweight aggregate. However, we could not get better result than control mixture; it might be because of less restraining property of fine LWA **[33]**.

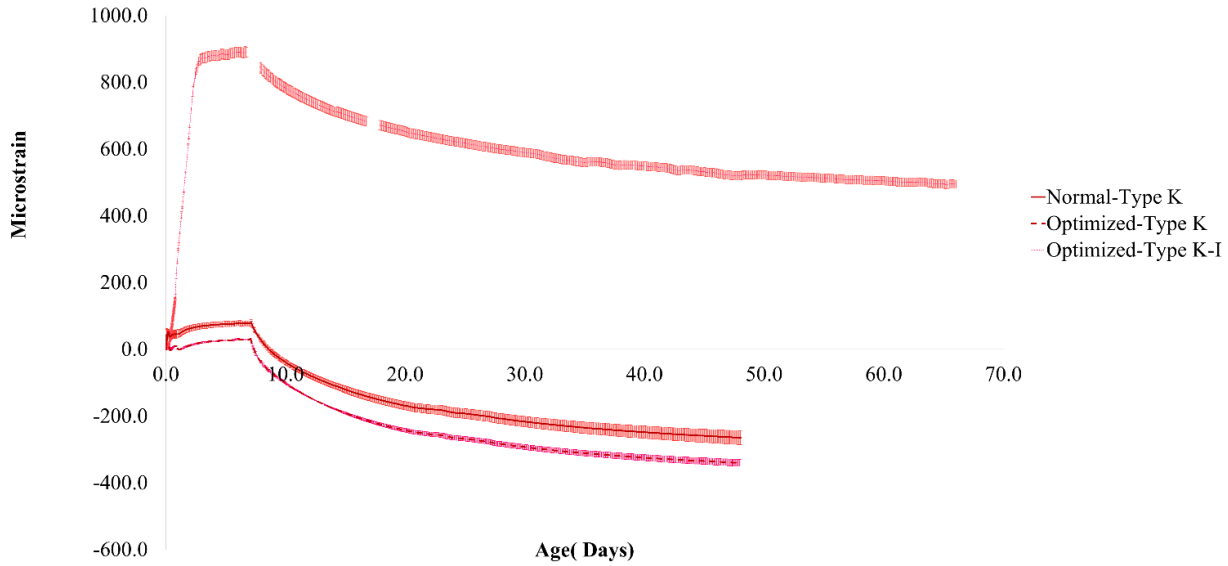

Figure 4.2. The strain change over time for the Type K mixtures.

As per **[11, 12]**, Type K is expected to have expansion initially and shrinkage as control mixtures. Then, it is expected to have shrinkage later as much as that of control mixture. However only one particular Type K mix showed an increased amount of expansion, otherwise it is almost similar to other control mixture design.

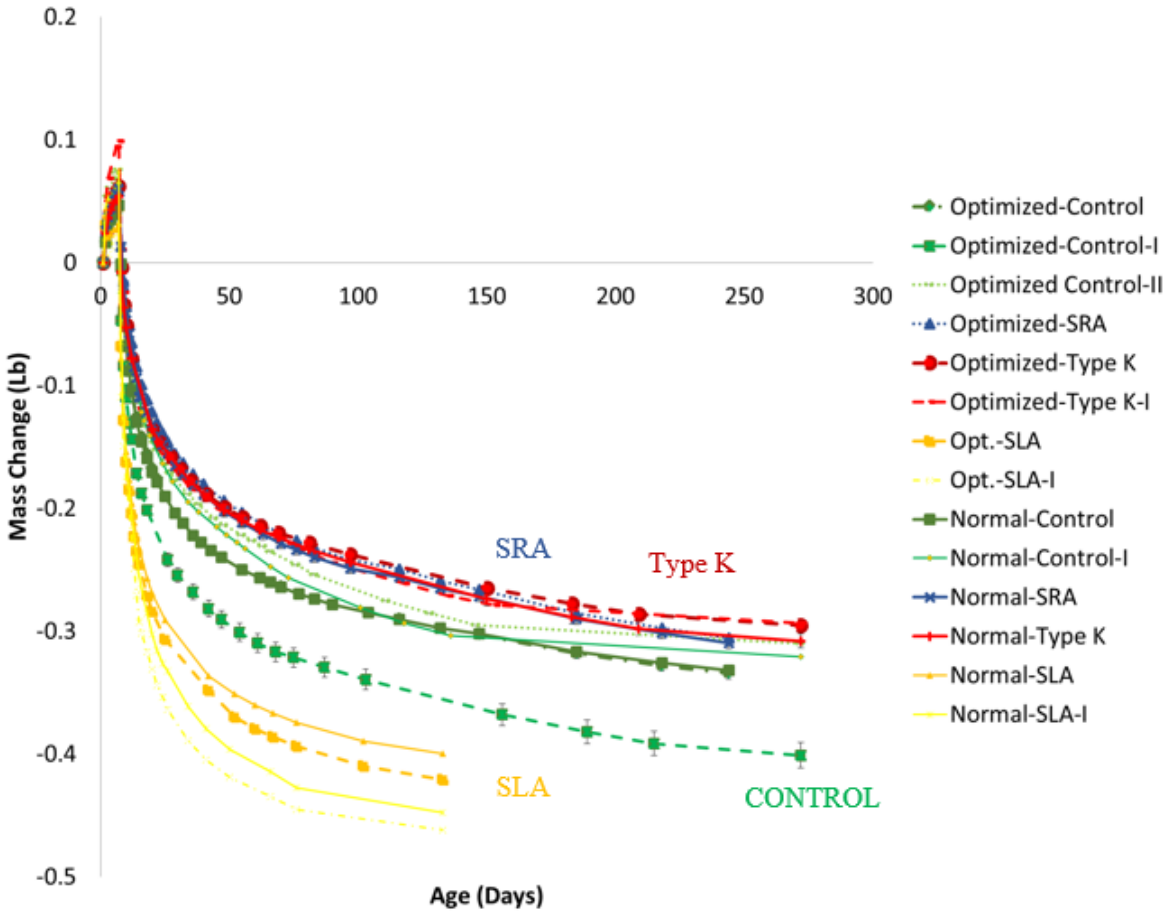

Figure 4.3. Mass Loss Graph

The graph shows SRA and Type K samples with similar mass loss. SLA sample has the highest moisture loss, then control samples, then SRA and type K. Mass gain occurs due to hydration and mass loss occurs due to drying. Since, the specimen is losing moisture from all the sides, after 7 days, the slope of mass change is large indicating significant loss of moisture. Moisture loss depends upon the porosity of the concrete.

So, the above graph shows that SRA and type K mixture had a similar mass loss. Still control specimen is showing similar but little more mass loss than previous two. In comparison to all of these, SLA specimen are losing larger amounts of moisture. As per (Weiss,1999), **[34]** there will not be much difference in mass loss due to control mixture and SRA mixture..

In the early stage of drying, the lost water mainly comes from the large capillary pores**[35]**. This supports that SLA sample which has lots of fine LWA having large void, lost water quickly in the initial phase, which is indicated by sharp down ward slope.

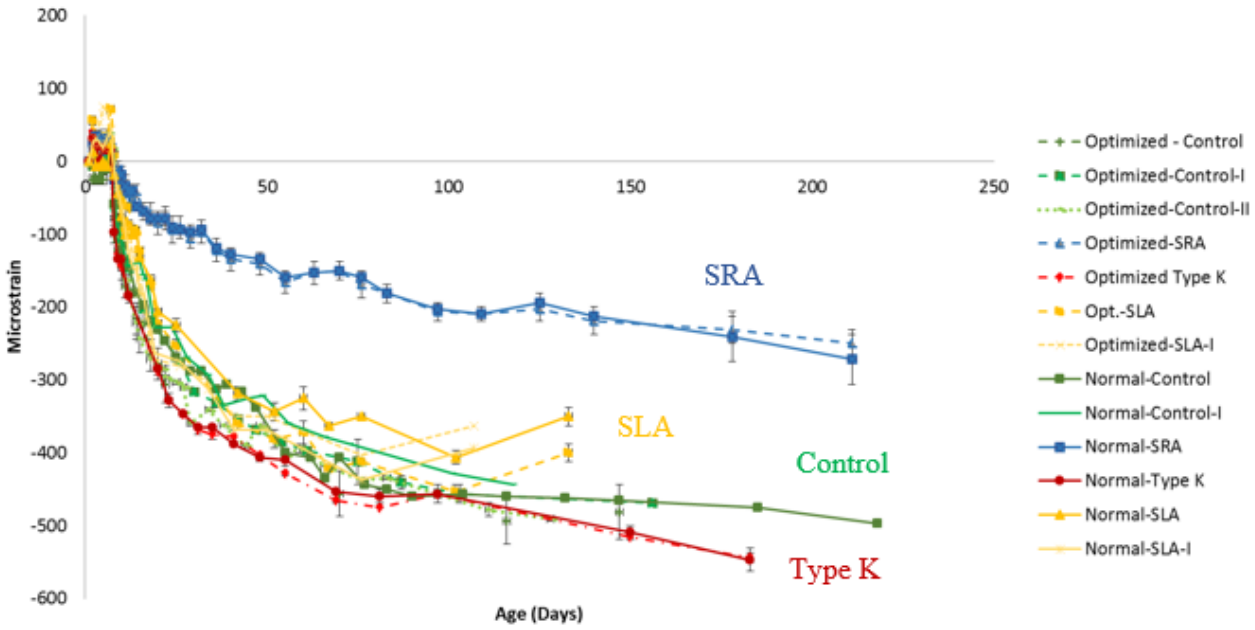

Figure 4.4 Strain change over time for the mixtures investigated as measured by axial comparator. Note: One Type K mixture is not shown. All the mixture are shown individually as well, so that all can be clearly understood

Though shrinkage measured with VBWG and comparator should be comparable, shrinkage measured with comparator shows more shrinkage if we compare the figure 3.1 with figure 3.4. This is because the shrinkage measured with comparator excludes 1 day expansion of the concrete. This verifies the importance of taking reading from very beginning. In addition, it might

be because in previous one, VBWG is kept inside, at the middle of the sample while in latter case pins are inserted at the end of the beam.

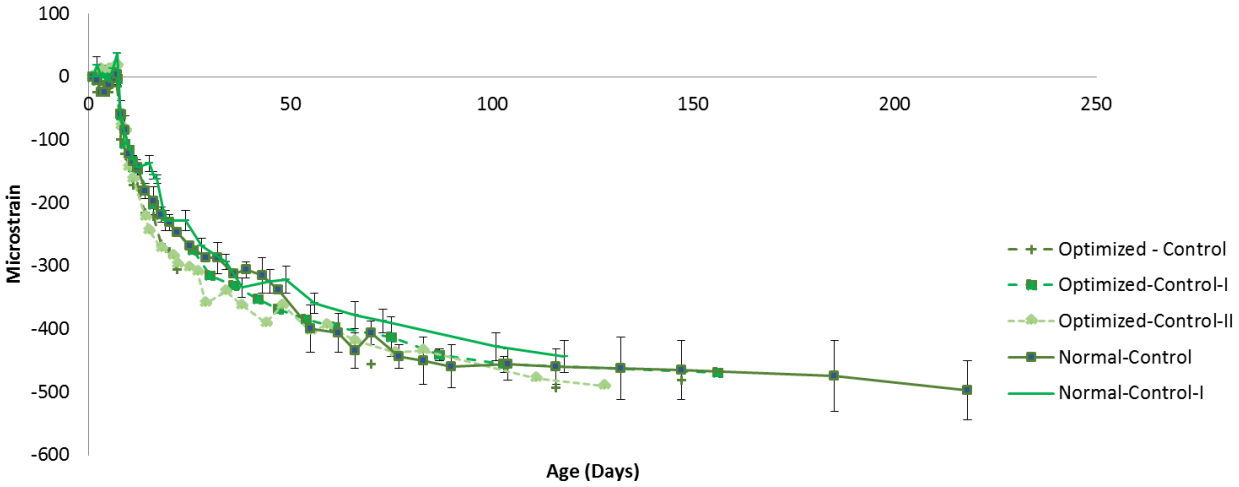

Figure 4.4 (a) Strain change over time for the mixtures investigated as measured by axial comparator for all Control Samples

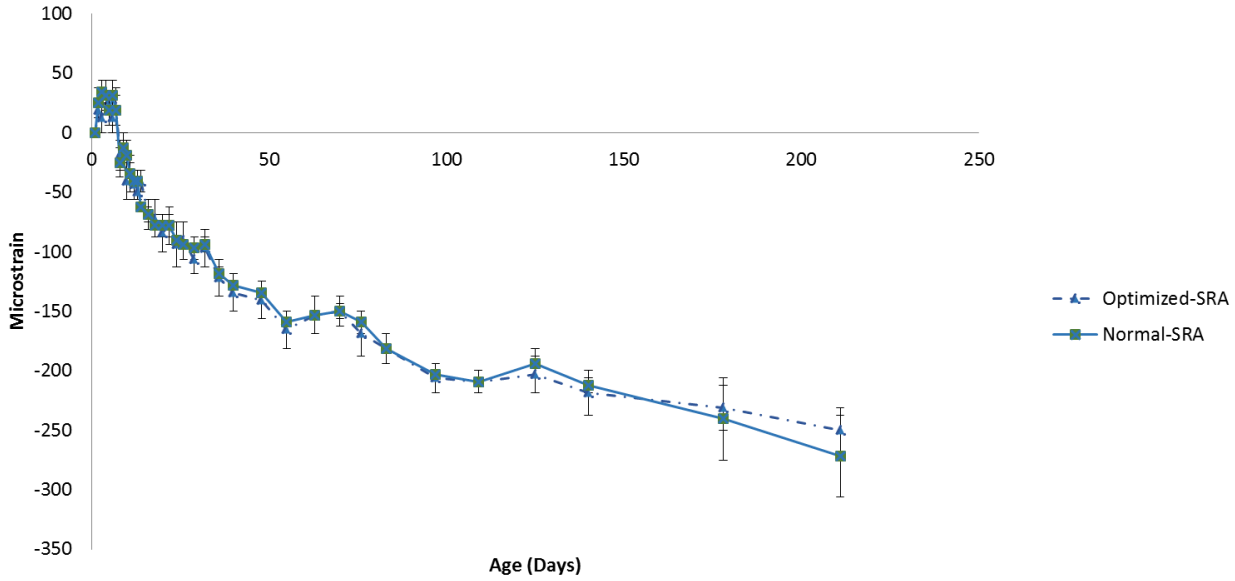

Figure 4.4 (b) Strain change over time for the mixtures investigated as measured by axial comparator for all SRA Samples

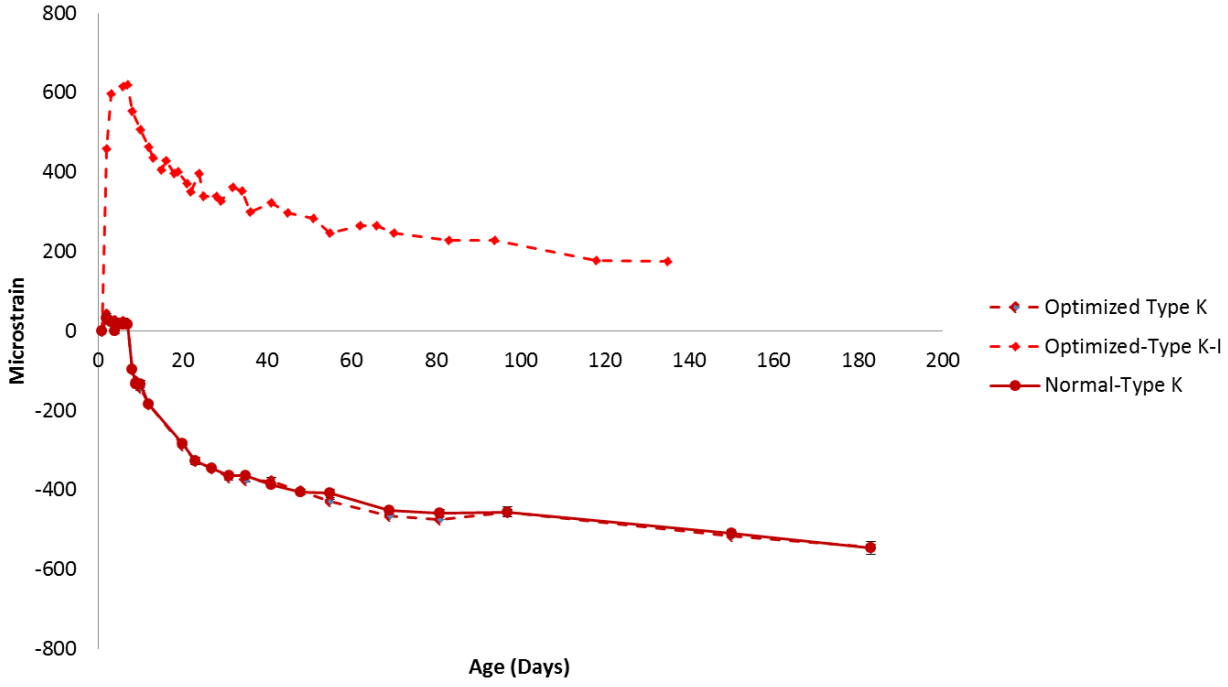

Figure 4.4 (c) Strain change over time for the mixtures investigated as measured by axial comparator for all Type K Samples

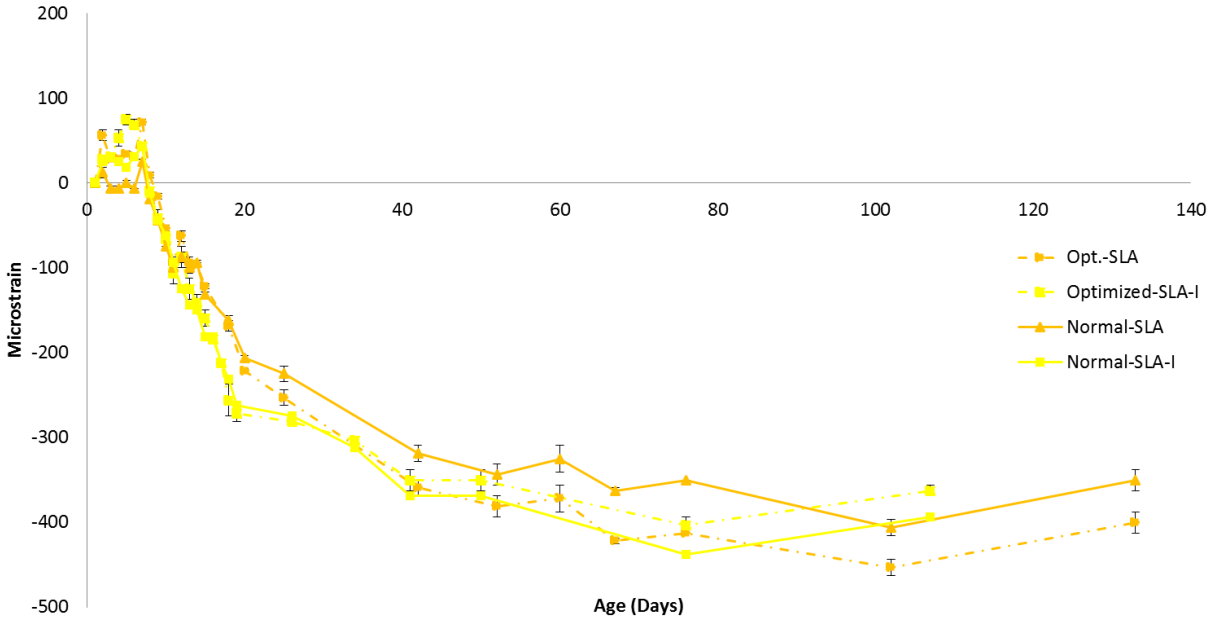

Figure 4.4 (d) Strain change over time for the mixtures investigated as measured by axial comparator for all SLA Samples

Curling Beam: Because of time and cost, not all the repeated mixtures used curling beam measurements.

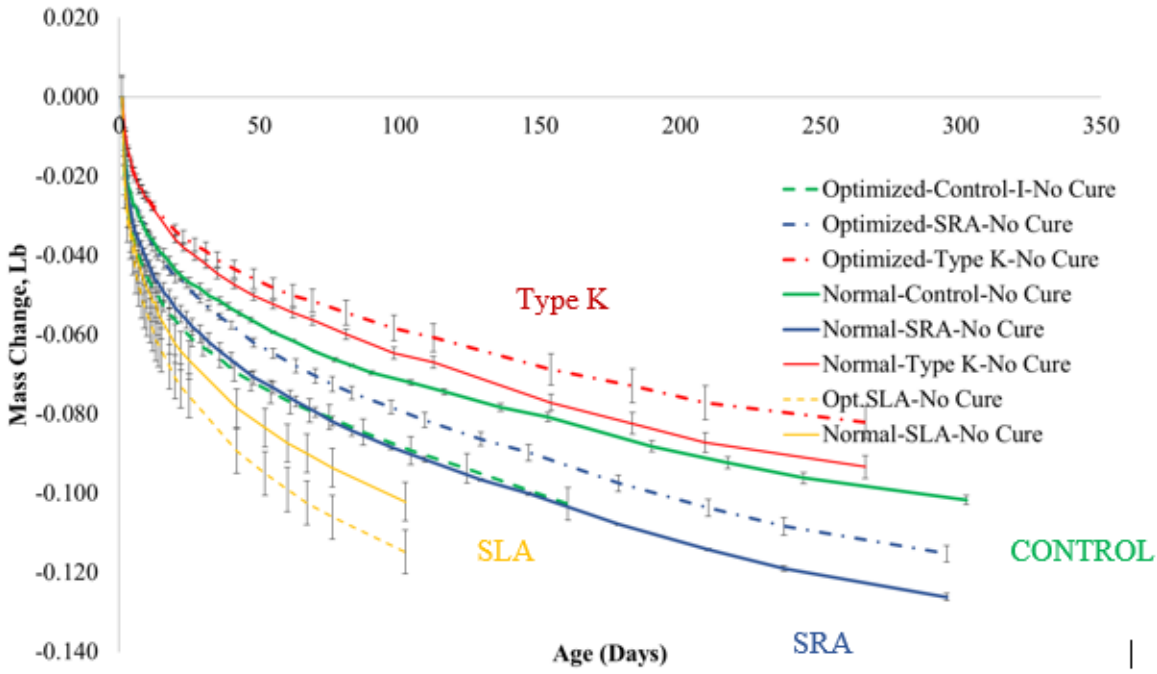

Figure 5.1 Mass changes over time for the no cure for all mixtures.
(Wherever there is optimized control-I, it is the repeated optimized control mix.)

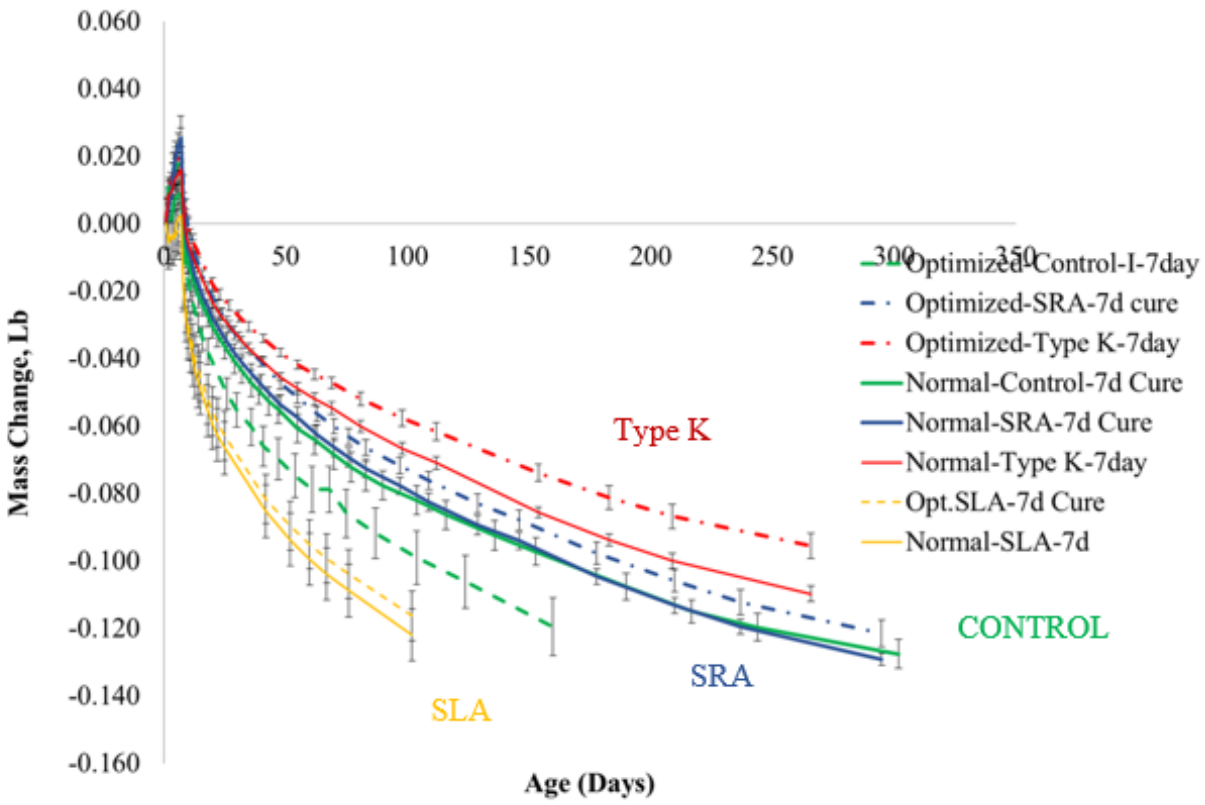

Figure 5.2 Mass changes over time for the all 7 day cure all mixtures.

(Wherever there is optimized control-I, it is the repeated optimized control mix.)

It is obvious to have different mass loss from curling beam than that of free shrinkage axial beam: one reason is that curling beam has only one open side to loose moisture and another reason is they have multiple faces.

The pattern of mass loss for both no cure and 7 day wet cure are similar.

The SLA concrete is losing high amount of moisture as free shrinking axial beam. The reason is same as earlier. SLA sample which has lots of fine LWA having large void, lost water quickly in the initial phase, which is indicated by sharp down ward slope.

In both the cases, SRA and control mixture shows similar moisture loss. While this is different from free shrinkage beam, where SRA has similar mass loss as Type K and then followed by control and SLA.

For curling shrinkage, first I have plotted the graphs showing comparison of shrinkage among all the mixtures at particular depths. Afterwards, for further discussion I have tried to compare curling shrinkage at different depths among all the mixtures at particular age – i.e. day 7, day 30 and day 100 only.

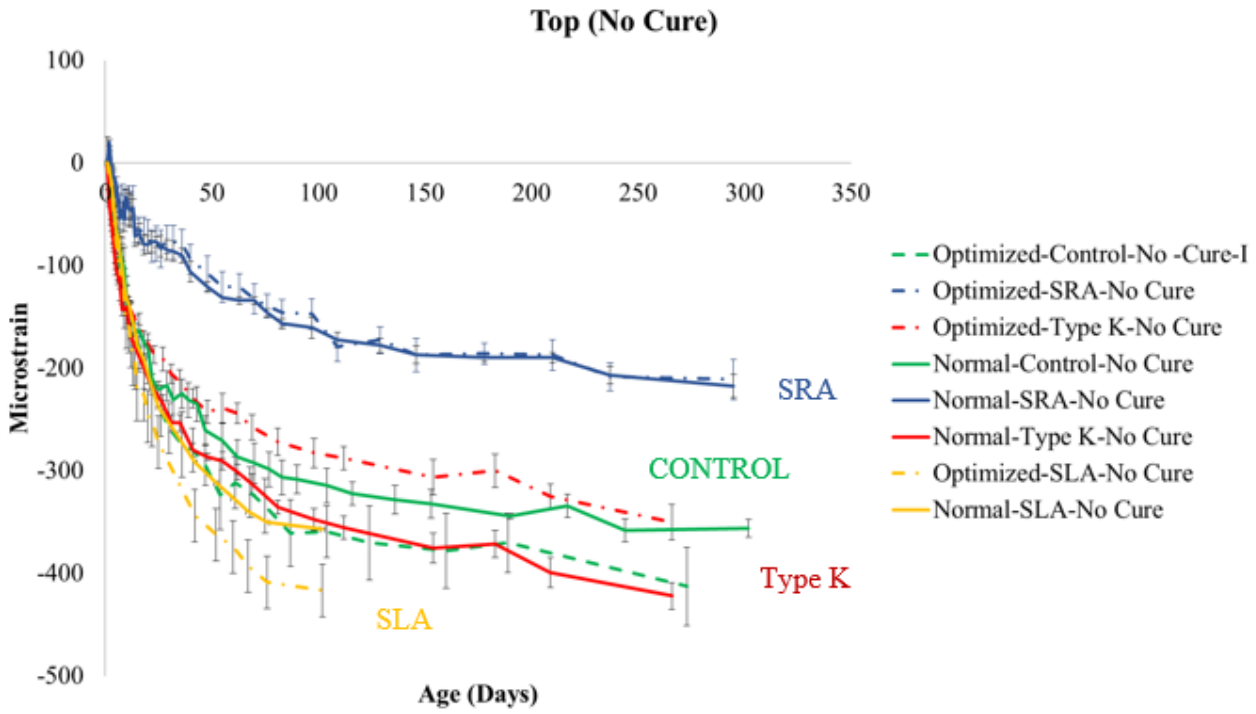

Figure 5.3 Strain changes at top level of curling beam over time for the no cure for all mixtures. (Wherever there is optimized control-I, it is the repeated optimized control mix.)

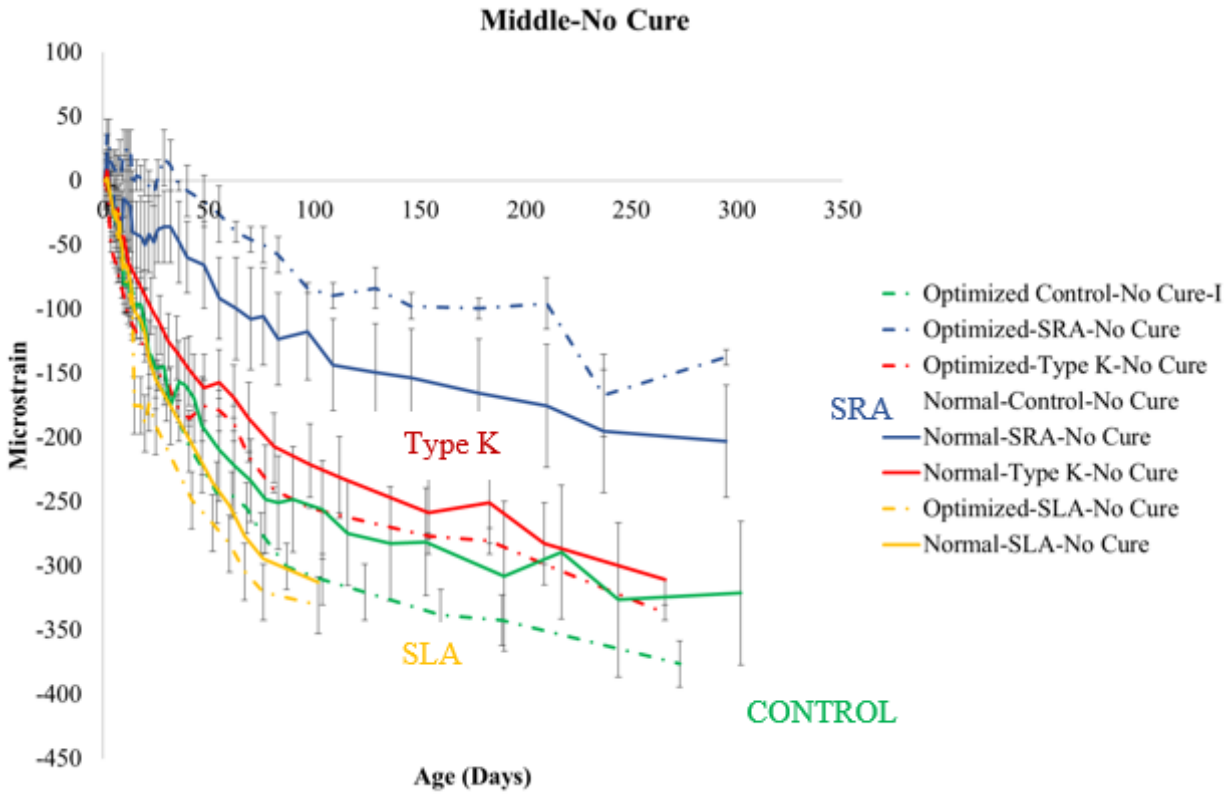

Figure 5.4 Strain changes at middle level of curling beam over time for the no cure for all mixtures.

(Wherever there is optimized control-I, it is the repeated optimized control mix.)

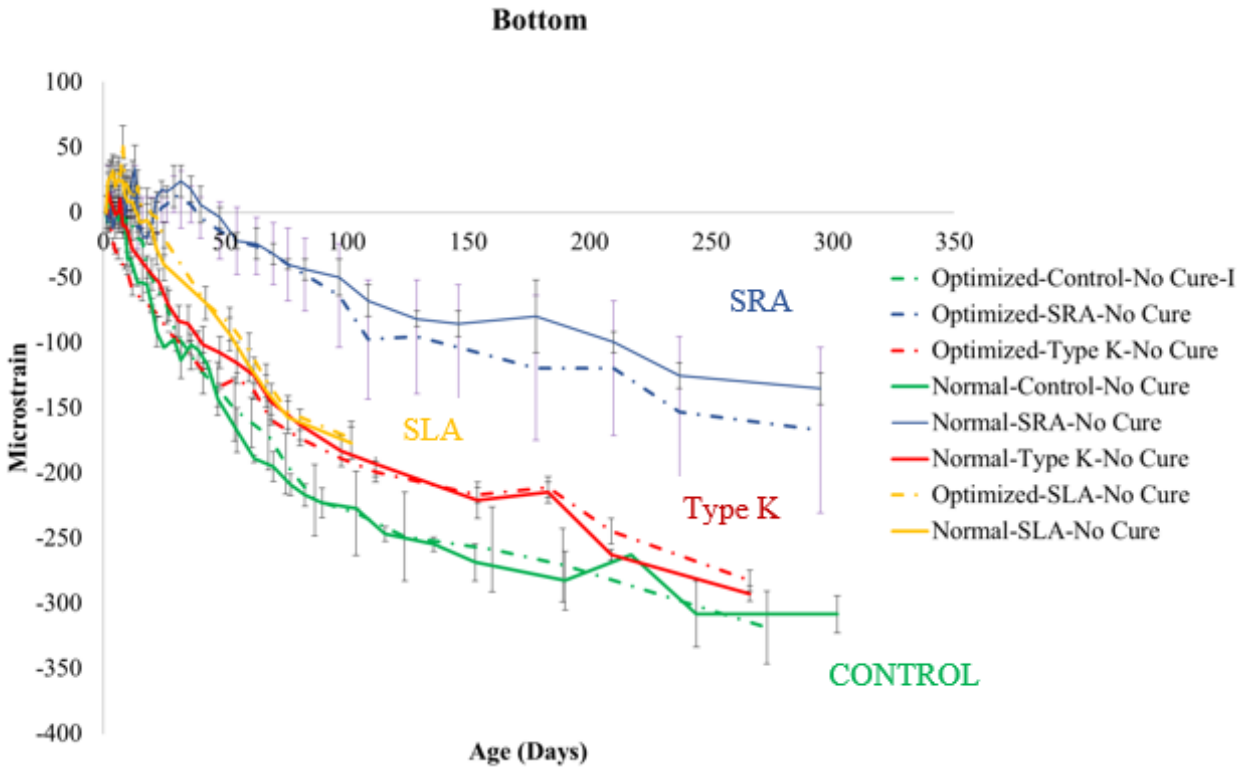

Figure 5.5 Strain changes at bottom level of curling beam over time for the no cure for all mixtures.
(Wherever there is optimized control-I, it is the repeated optimized control mix.)

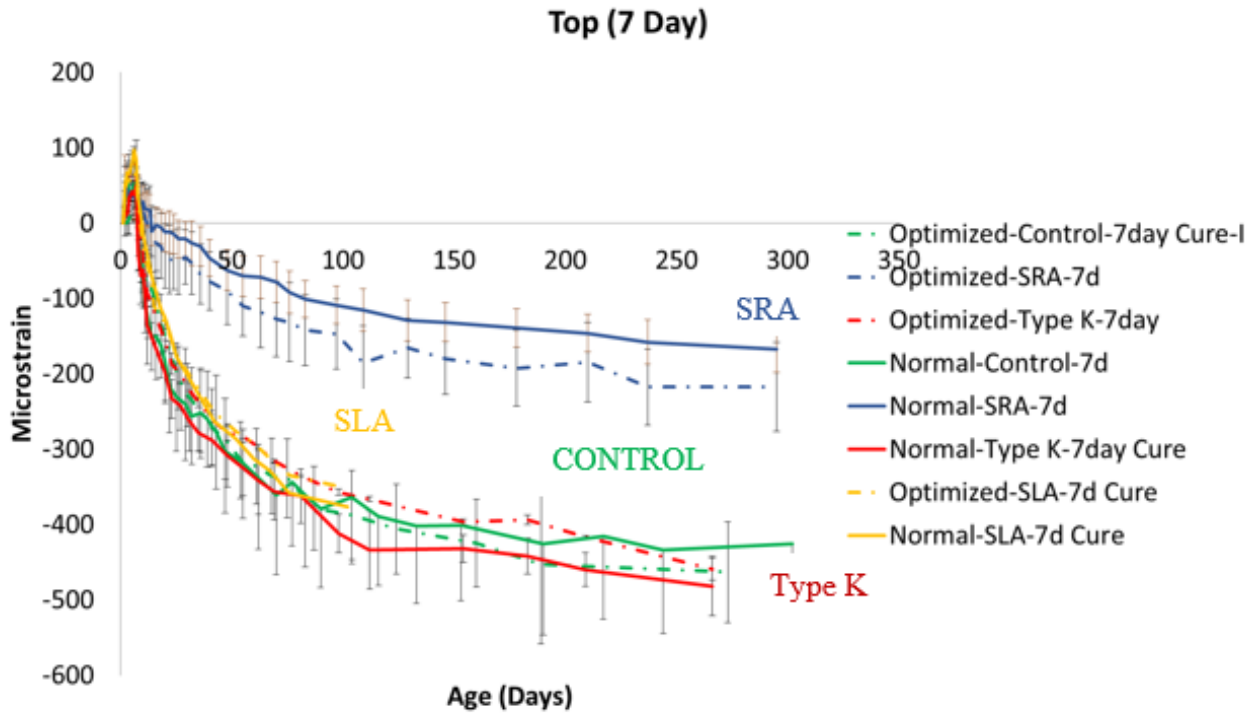

Figure 5.6 Strain changes at top level of curling beam over time for all 7-day cure. (Wherever there is optimized control-I, it is the repeated optimized control mix.)

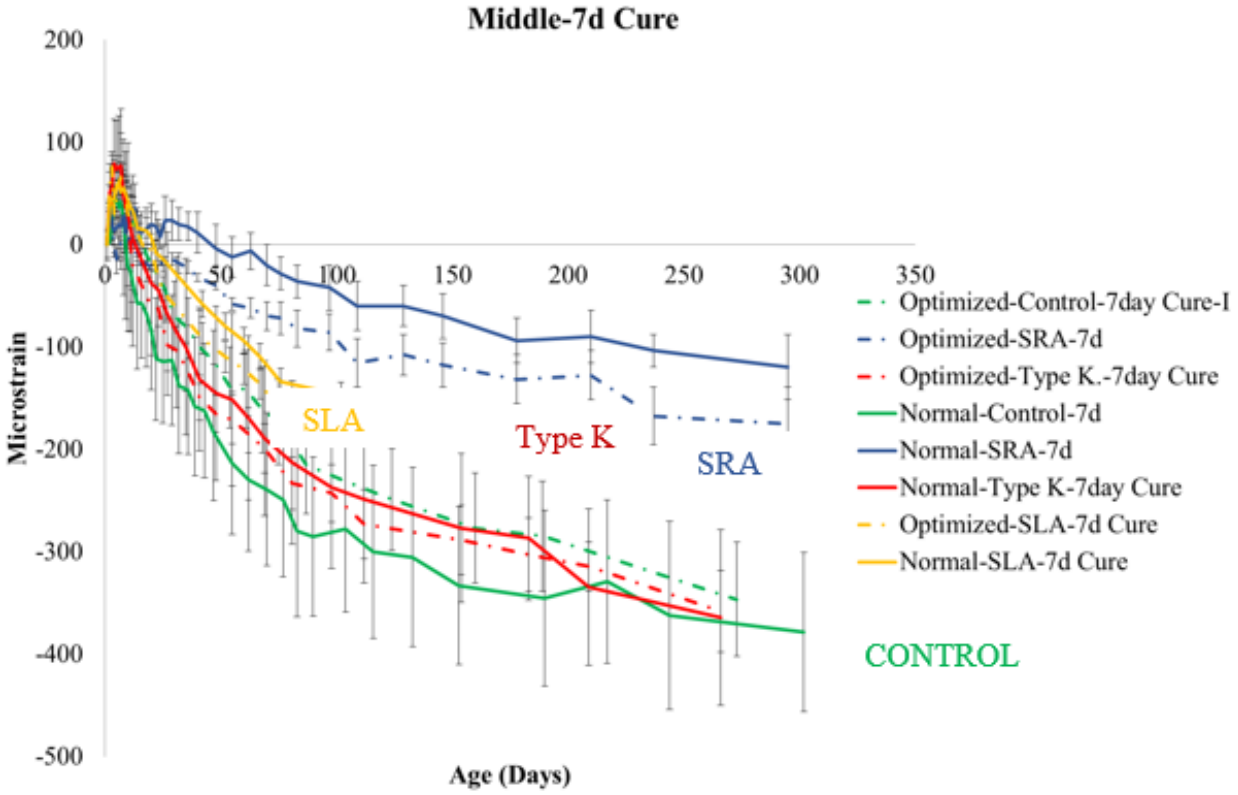

Figure 5.7 Strain changes at middle level of curling beam over time for all 7-day cure. *(Wherever there is optimized control-I, it is the repeated optimized control mix.)*

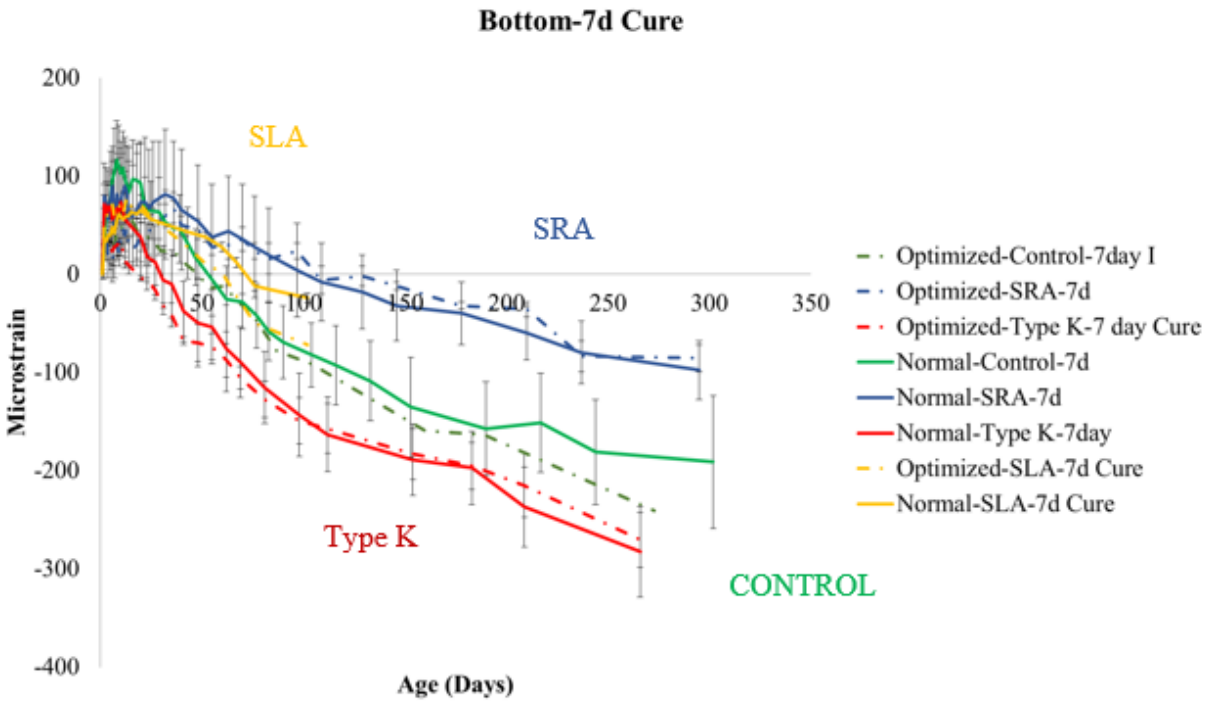

Figure 5.8 Strain changes at bottom level of curling beam over time for all 7-day cure. (Wherever there is optimized control-I, it is the repeated optimized control mix.)

As expected **[24]**, 7day cured samples for every batch shows higher curling shrinkage as compared with no cured samples.

After 100 days, the difference in strain from top with bottom for no cure-optimized control is 130 micro strain, no cure Normal control has 100 micro strain, 7-day cure optimized control is 300 micro strain and 7-day cure Normal control has 280 micro strain.

SRA reduces curling **[7]**, which agrees with our findings too. The difference in strain from top with bottom for no cure optimized SRA is 110 micro strain, no cure Normal SRA has 110 micro strain, 7-day cure optimized SRA has 180 micro strain and 7-day cure Normal SRA has 160 micro strain at 100 days.

Similarly, at 100 day, the difference in strain from top with bottom for no cure-optimized Type K is 240 micro strain, no cure Normal Type K has 180 micro strain, 7-day cure optimized Type K has 280 micro strain and 7-day cure Normal Type K has 320 micro strain.

Likewise, at 100 day, the difference in strain from top with bottom for no cure-optimized SLA is 240 micro strain, no cure Normal SLA has 180 micro strain, 7-day cure optimized SLA is 280 micro strain and 7-day cure Normal SLA has 320 micro strain.

I have presented all these differences between top and bottom strains in order to indicate that there is strain gradient. For further discussion, I have plotted the graph by taking the strains at different depth. Following are the graphs for that.

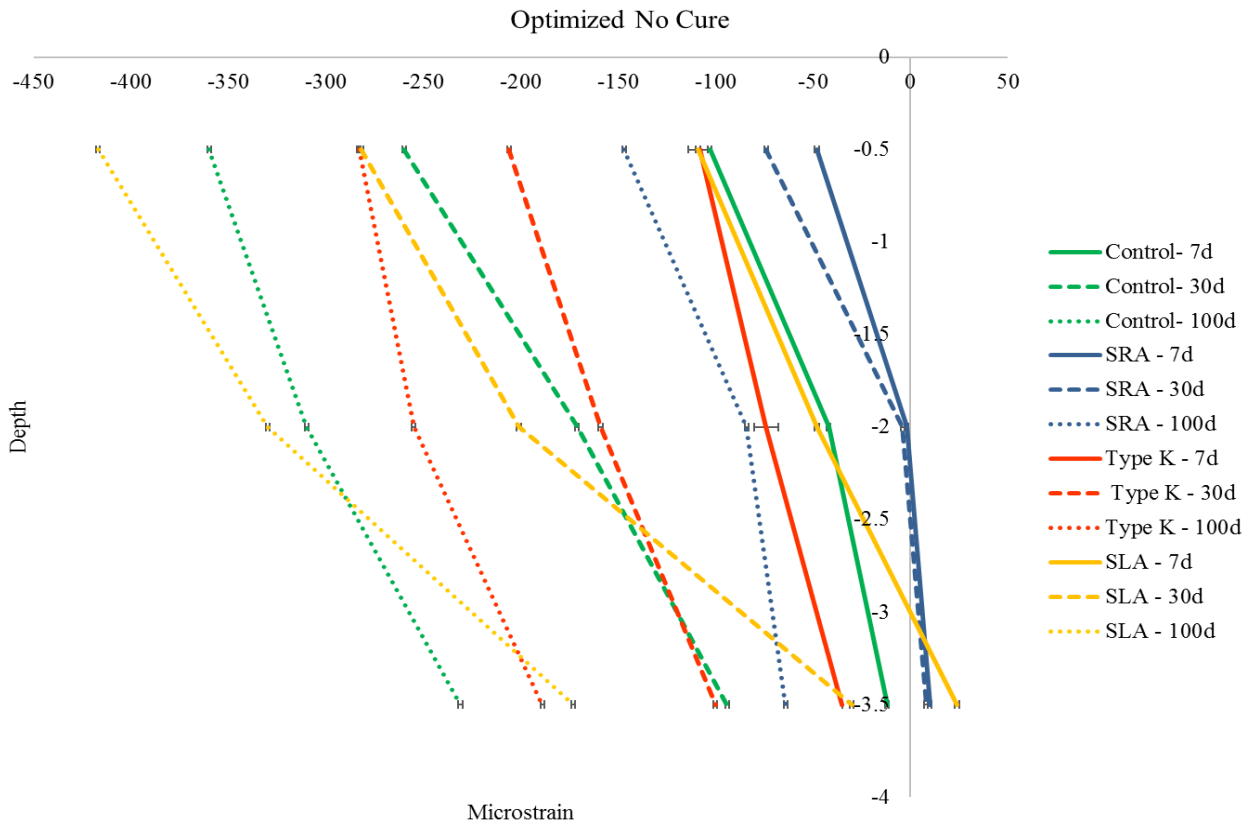

Figure 5.10: showing strain gradient at different depth for optimized no cure over time

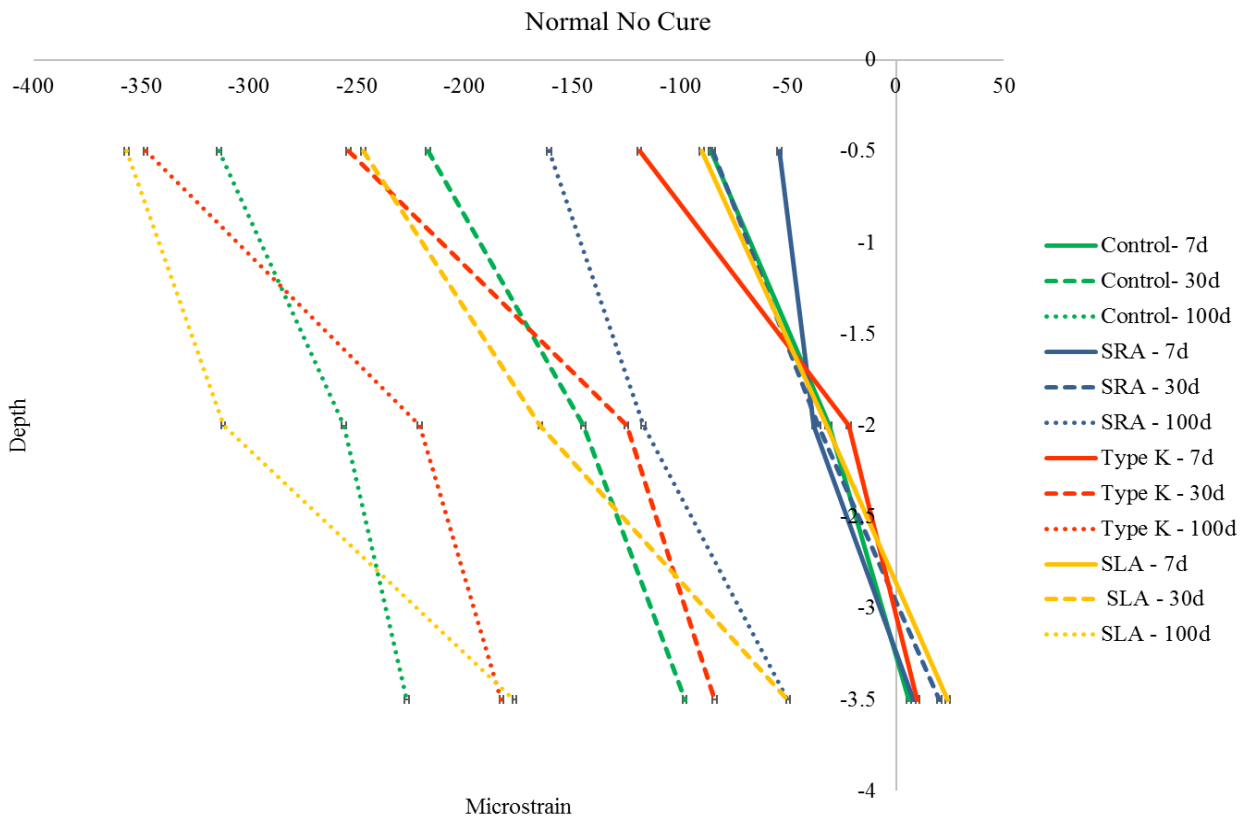

Figure 5.11: showing strain gradient at different depth for normal no cure over time

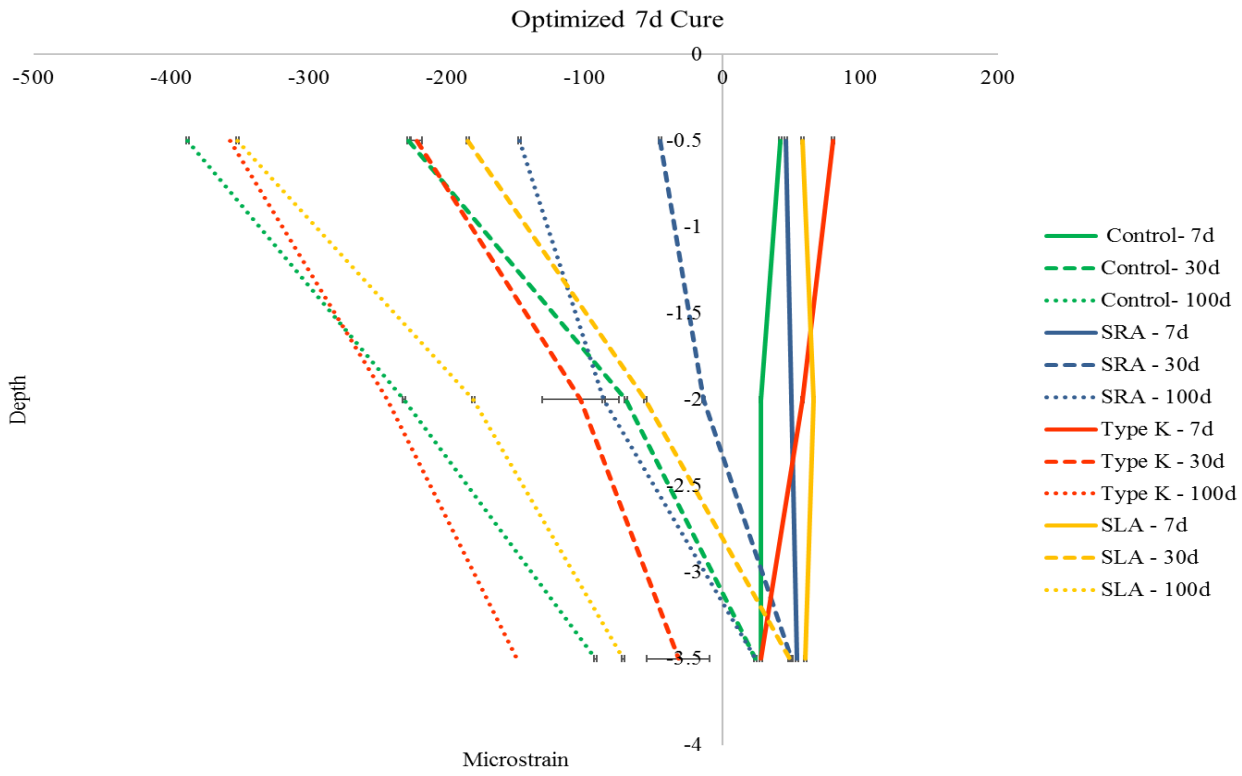

Figure 5.12: showing strain gradient at different depth for optimized 7 days cure over time

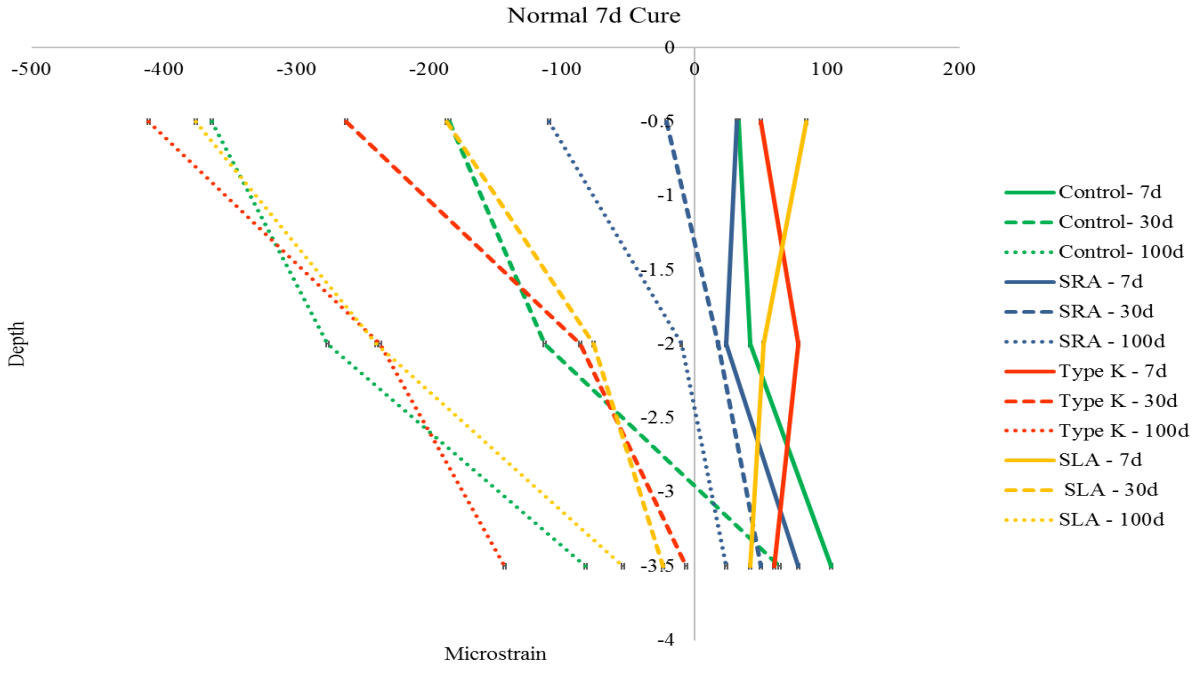

Figure 5.13: showing strain gradient at different depth for normal 7 days cure over time

Figure 5.10-5.13 shows that strain at 0.5” is higher than strain at 2” and 3.5” depth.

For no cure sample, the shrinkage starts from the beginning whereas for 7days wet cure samples, shrinkage starts after curing.

As in case of axial shrinkage, SRA showed less shrinkage at all depths as compared to all other mixtures. Furthermore, SRA is showing less curl in comparison to other mixture if we look above graphs. However, the curling performance is not that promising as that in case of axial shrinkage.

The inclination of 7 days cured samples were steeper than those of no cure samples. It can be seen distinct if we look at 100-day results. For no cure samples, SLA is showing more curling shrinkage followed by control, type K and SRA samples. For 7 day cure, optimized SLA is showing less curling shrinkage after SRA and all other three are showing similar trend and similar shrinkage.

Furthermore, relative humidity graphs later, will support these results.

Internal Relative Humidity:

In order to support the strain changes relative humidity is measured at same level, starting from 5th day of casting the samples.

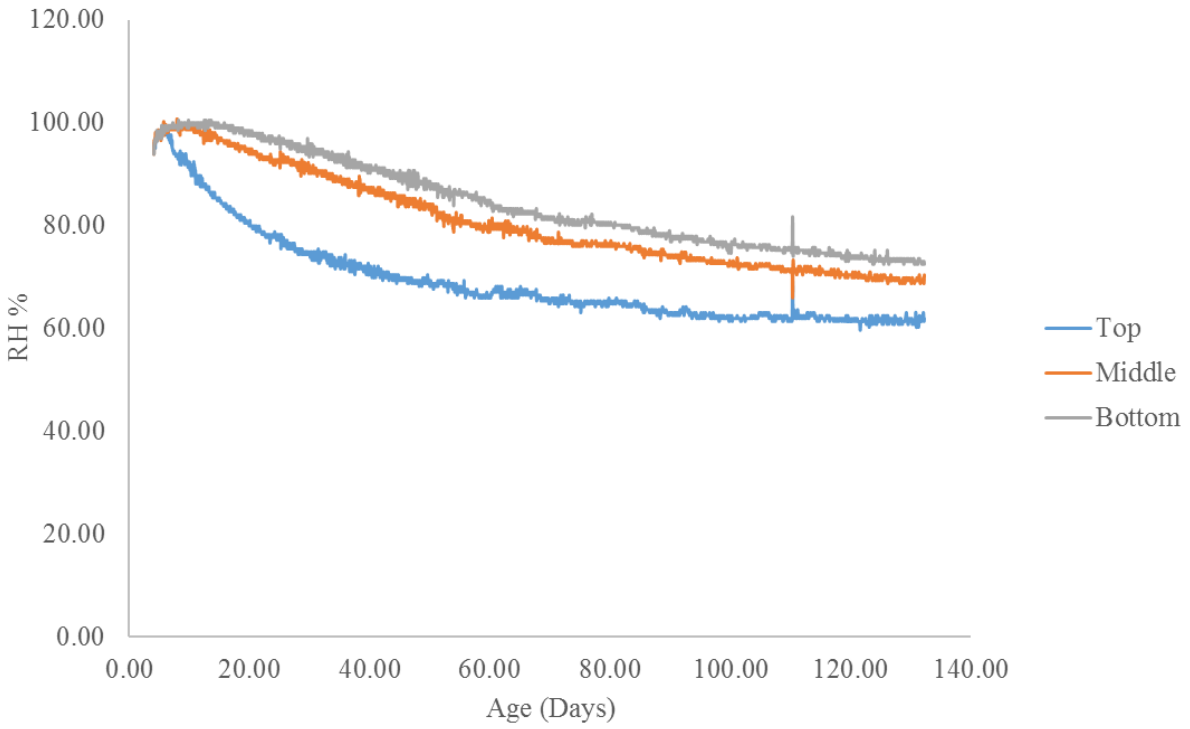

Figure 5.14: showing typical RH humidity change over time

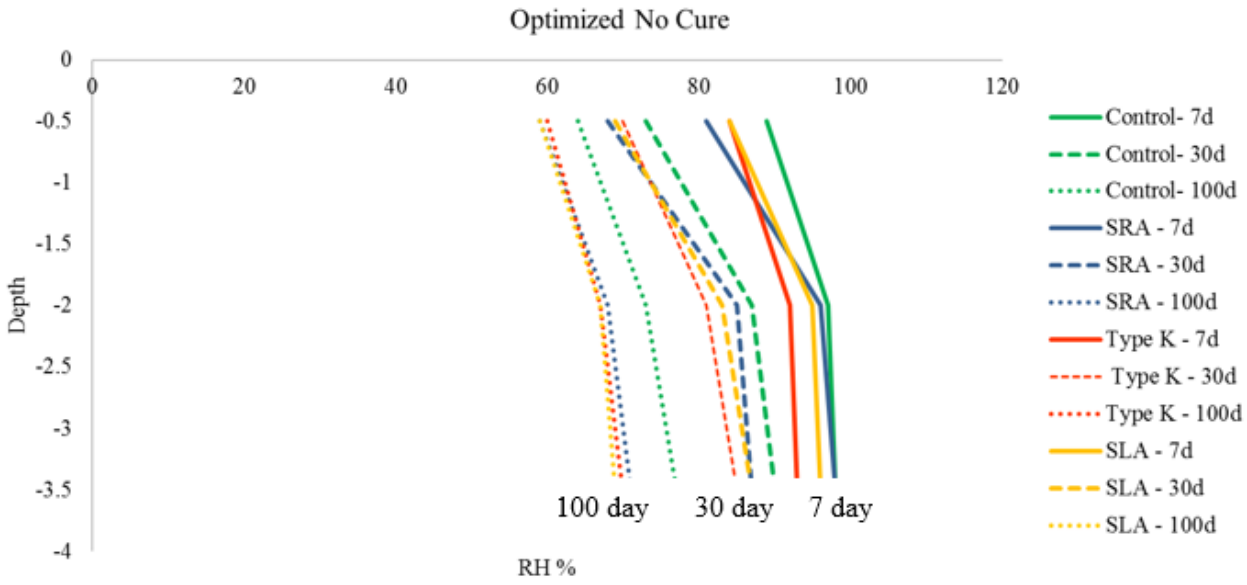

Figure 5.15: showing gradient in RH at different depth for optimized no cure over time

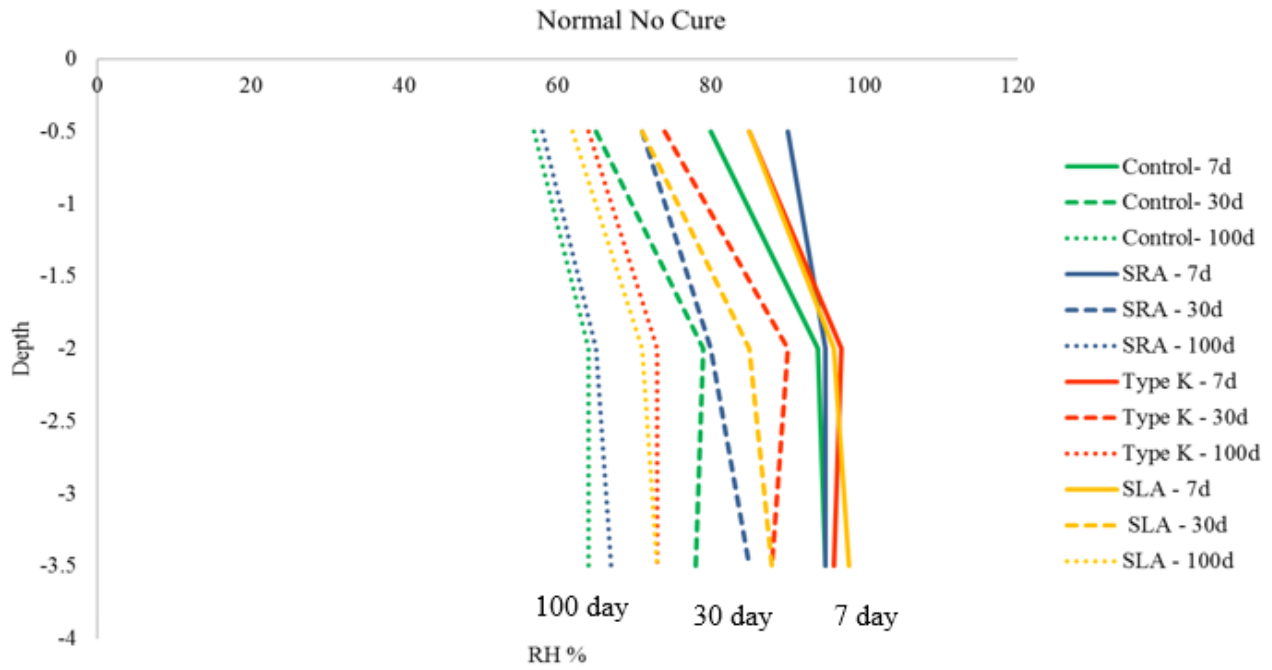

Figure 5.16: showing gradient in RH at different depth for optimized 7 days cure over time

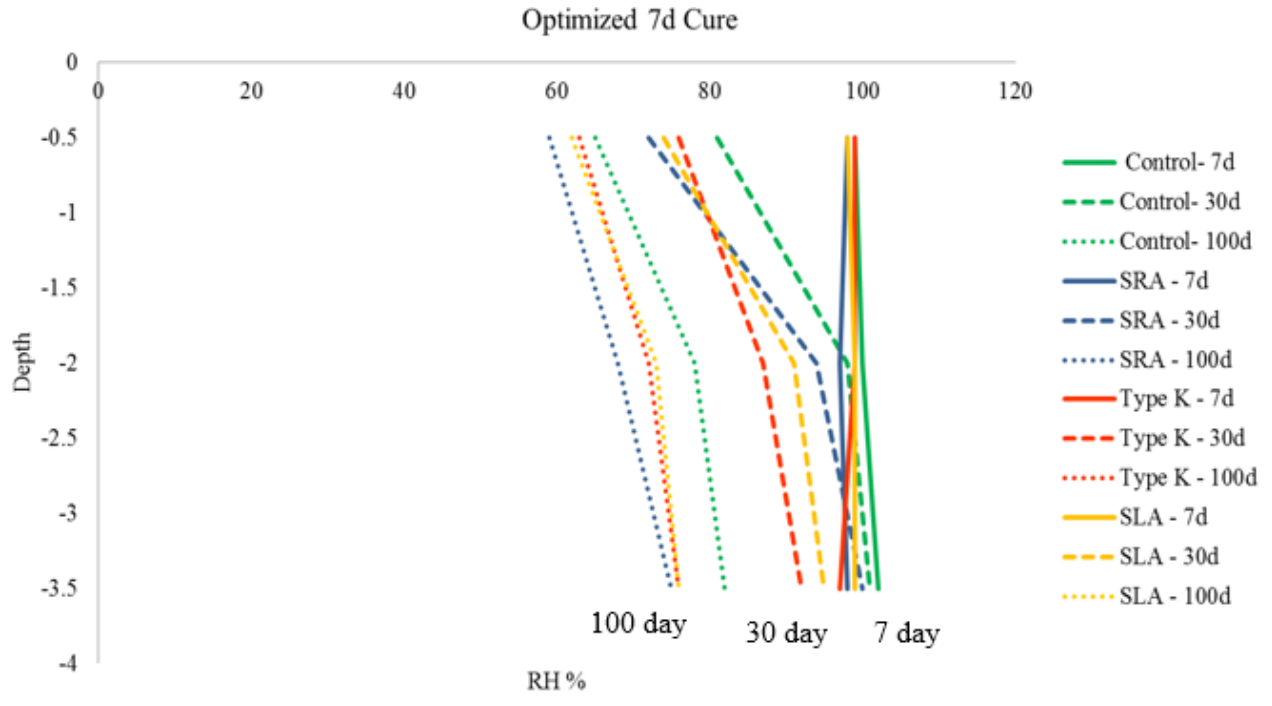

Figure 5.17: showing gradient in RH at different depth for normal no cure over time

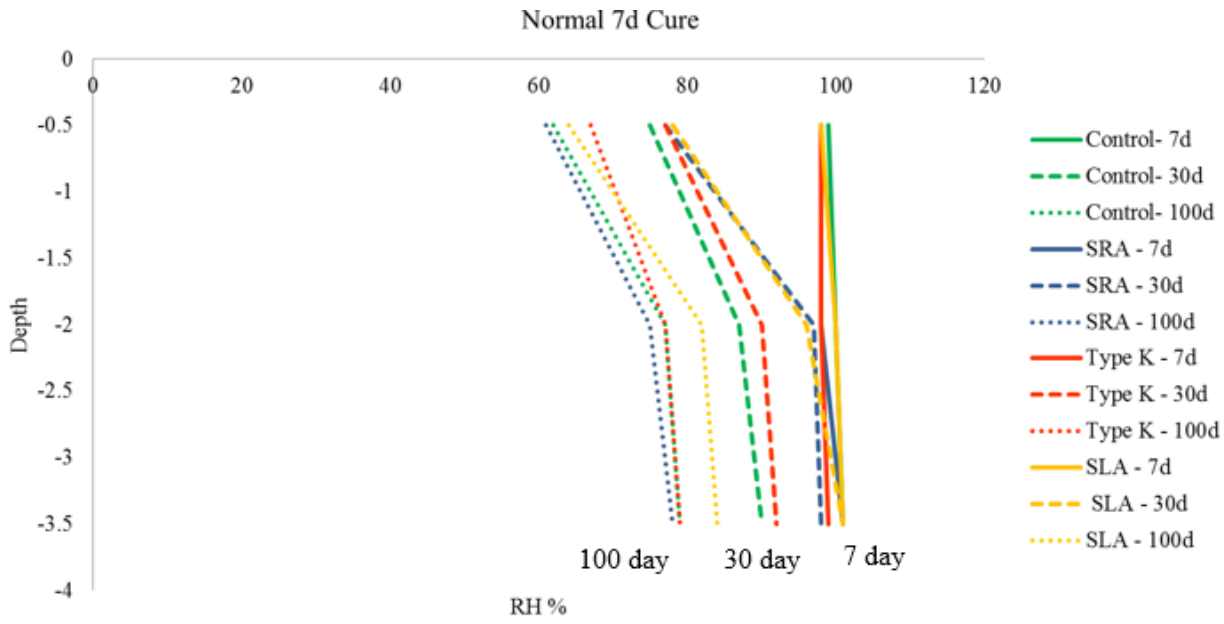

Figure 5.18 showing gradient in RH at different depth for normal 7-day cure over time

Figure 5.10-5.13 shows that RH at 0.5" is lesser than RH at 2" and 3.5" depth. The relative humidty at 2" and 3.5" are somewhat similar.

For no cure sample, RH is decreasing from the beginning whereas for 7days wet cure samples, RH is decreasing later.

In case of optimized no cure mixture, all samples are showing similar trend of decreasing RH for 7 days and 30 days. However, there is less decrease in RH in case of control sample in 100 days as compared to other. In case of optimized 7 days cure, curvature of lines are observed to be more in 30 days than in 100 days and no curvature at all in case of 7 days. Control sample is showing less decrease in RH as in no cure optimized mixture. Normal no cure samples show similar trend of RH change from the beginning. While in case of normal 7days cured samples, there is little more curvature in 30days but that significant as in optimized mix.

These above graphs supports curling and mass loss in the beam. Thus, internal relative humidity data are important.

4.3.2 Mechanical Properties:

From these same mixtures cylinders to determine their corresponding mechanical properties. By comparing the strains from the shrinkage to the changes in modulus and strength then this can help predict the cracking of the concrete. Figure 5.1, Fig. 5.2, Fig. 5.3, and Fig. 5.4 shows the changes in the compressive strength, tension strength, static and dynamic modulus over time. All of these values show very similar trends with the Type K cement showing the highest values, the controls show the next highest value, and the SRA shows the lowest values. Graph shows less difference between optimized and non-optimized mix. Optimized Gradation uses less paste to coat around the aggregates than non-optimized graded and the mixtures show comparable results.

There seem to be some variation in the data for the modulus and splitting tension strength. This is likely caused by material variation in these tests.

I) Compressive Strength:

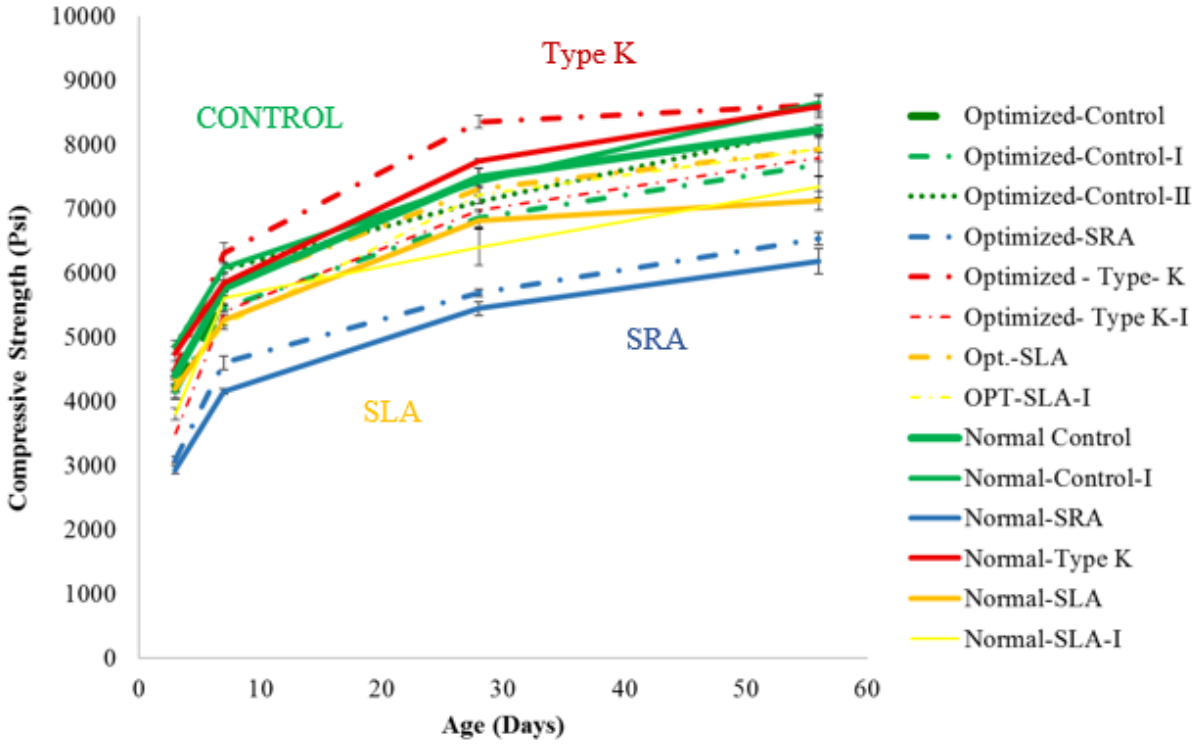

Figure 6.1 Compressive strength change over time for the different mixtures.

(Optimized-Type-K-I samples are tested only for compressive strength; other properties are not considered since strain changes of these samples are highly variable)

Almost all concrete mixes show similar trend in increase in compressive strength from 3 day to 7 day. Initially, when concrete is fresh, hydrates quickly than later. Again, concrete gains more strength. In about 28 days, concrete samples achieved majority of its serviceable strength. Afterwards, concrete gains strength slowly which are indicated by mild slope lines in the graph.

As expected, figure 5.1 shows that concrete mix with type K cement gained more compressive strength than control mixes, with SLA and with SRA. **[11, 12, 36]** Type K cement which has sulphoaluminate forms ettrignite (expansive material) during hydration. Ettrignite is needle like crystals, which add strength to the concrete.

Likewise, concrete mix with SRA shows lowest compressive strength out of all mixes because, SRA reduces the pore water pressure of water filled in the pores of concrete. It dilutes the paste and reduces the hydration **[7]**, which results in the reduction of the compressive strength **[6, 7]**. The early strength of concrete is decreased by more than 30% while 7day, 28 day strength by around 25% and has lesser effect on 56 day strength, it is about 20-25%. Such result is supported by other findings too **[6, 7]**.

The decrease in strength caused by the SRA may be of concern to many contractors and this may need to be addressed by lowering the design strength of a bridge deck that uses these materials. While a lower strength may seem like a negative it may actually play to the favor of the concrete. A lower compressive strength also means a lower modulus. This means that the stress the concrete experiences for a given strain is lower than a material with a higher modulus. This can

be helpful for reducing cracking as strains that are placed on the sample in early ages can be reduced by creep.

Surprisingly, SLA shows lower strength, though many literatures says lightweight aggregate provides similar strength even for high strength concrete. Whereas, Shin et.al.**[15]** found slightly decrease in compressive strength as well as other splitting tensile strength and modulus of elasticity.

II) Static Modulus:

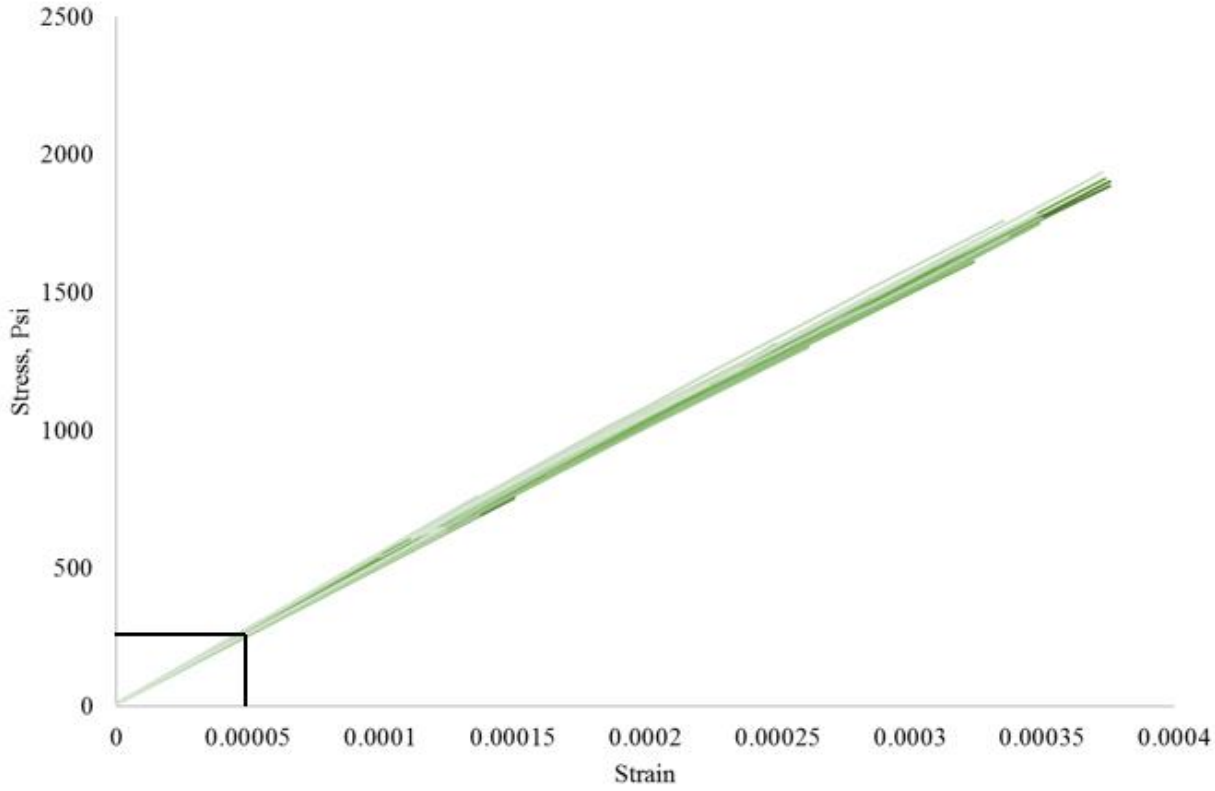

Figure 6.2 showing typical graph obtained from the static modulus test.

In this graph, there are twenty-four test results. The curves are close with each other, which indicates results are less variable. As the procedure discussed earlier in the methodology section, first set of values are taken at the five micro - strain and second set of values are taken at 40 % of

ultimate load from the graph in order to calculate static modulus of elasticity. In this way static modulus were calculated for all three samples from each mixture for 3, 7, 28 and 56 days. Finally, afterwards we come up with following graphs.

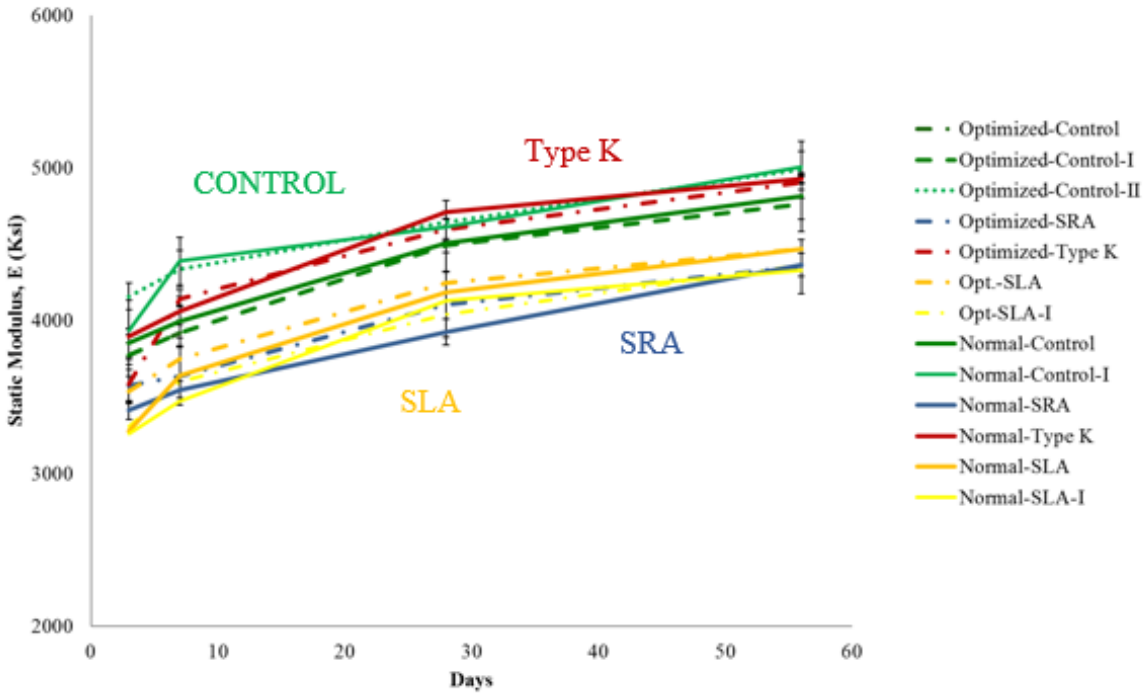

Figure 6.3 Static modulus change over time for the different mixtures.

The trend of graph is similar to the previous graph of compressive strength; concrete mix with type K cement on the top followed by control mixes, SLA mixes and then SRA mixes. This makes sense because static modulus is correlated to compressive strength. Since, low static modulus is desirable for mitigating cracking, SRA is best and then SLA. For an illustration:

$$\text{Modulus of Elasticity (E)} = \frac{\textbf{Stress } (\boldsymbol{\sigma})}{\textbf{Strain} (\boldsymbol{\varepsilon})}$$

If we have same strain but less modulus then we will get less amount of stress. From our shrinkage graph, we are getting both less strain and less modulus for SRA; thus, SRA will have

less stress. While SLA has similar strain like those of control samples but less modulus, thus, we can have less stress than control sample.

When, the static modulus obtained from the experiments were compared with that of theoretical values then the results are more or less similar. Here are few graphs for that.

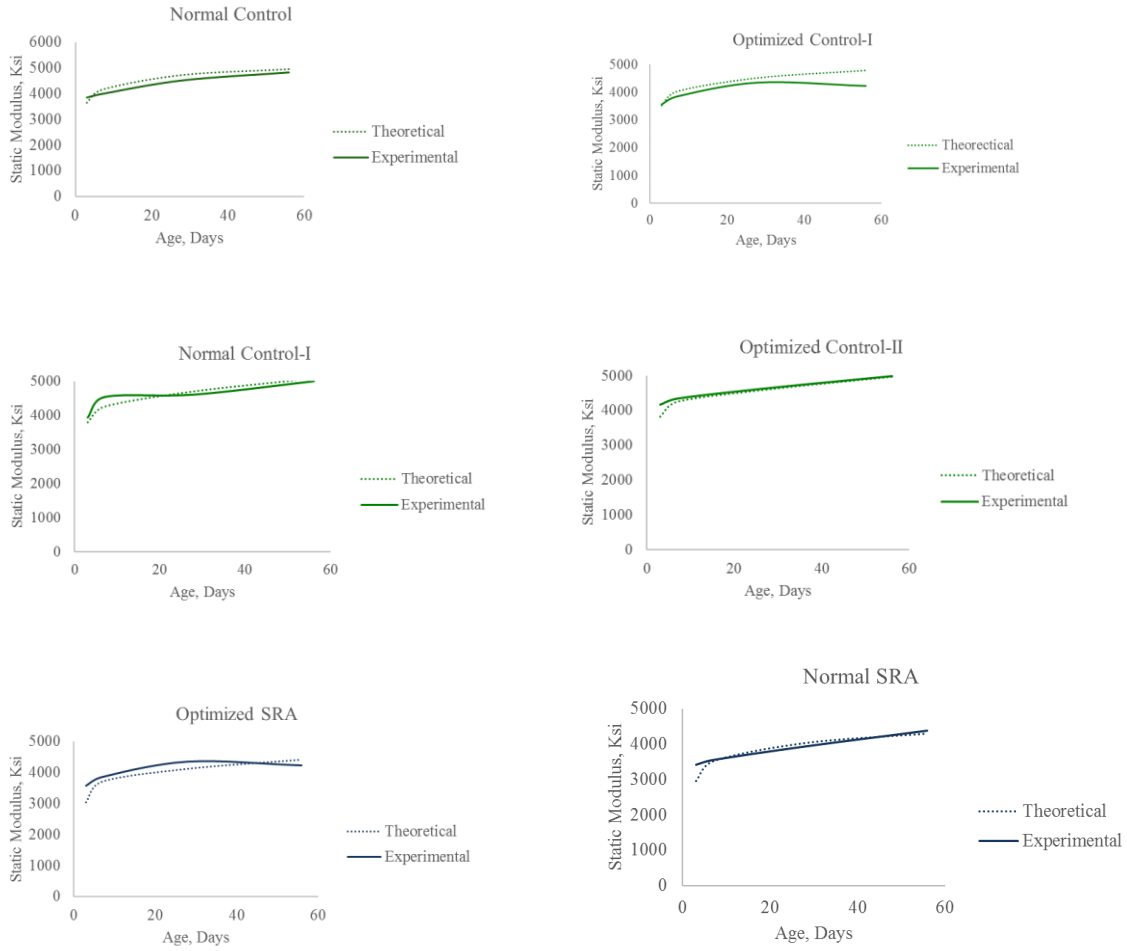

Figure 6.3 (a) Comparision between Theoretical Static Modulus with Experimental Static Modulus

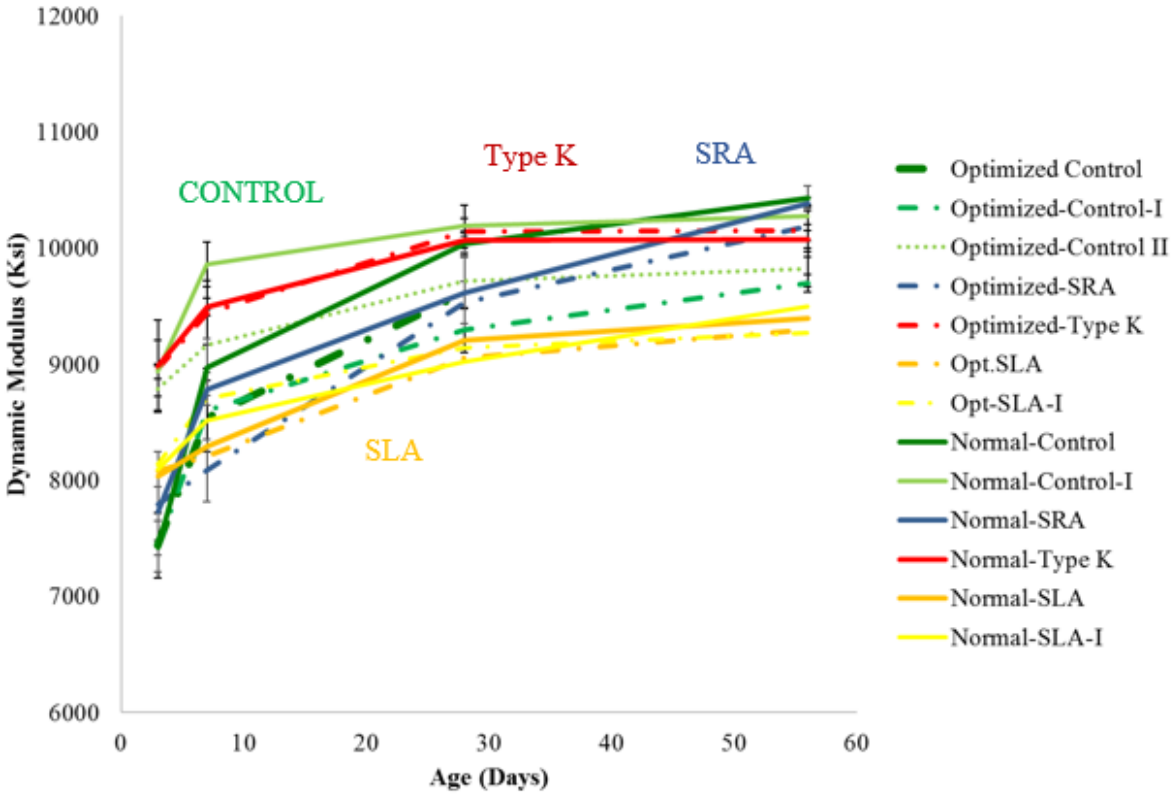

Figure 6.3 Dynamic Modulus change over time for different mixtures

If we compare the static modulus of elasticity (E_s) with dynamic modulus (E_d) from Figure 4.2 and 4.3, dynamic modulus is more than two times. Few literatures suggests variable results, varying from 1.1 to 2 times **[37]** and suggested that it depends upon the aggregate type i.e. dolomitic limestone would have different dynamic modulus as compared to that of schist and granite.

Above figure 6.3 shows SLA with lowest dynamic modulus, which is great, we need to have that. For an illustration:

Modulus of Elasticity (E) = $\frac{\text{Stress } (\sigma)}{\text{Strain}(\varepsilon)}$

If we have same strain but less modulus then we will get less amount of stress as in case of static modulus. While SLA has similar strain like those of control samples but less modulus, thus, we can have less stress than control sample.

Meanwhile, SRA is showing surprisingly high dynamic modulus than that of SLA sample and both optimized and non-optimized concrete are close enough. However, control samples are giving random results. While Type K samples are quite in same trend as in static modulus.

The reason behind sporadically random results are: it is quite difficult to determine first transit time accurately, second it depends on moisture content of samples, third the quality and quantity of coupling agent used in the testing.

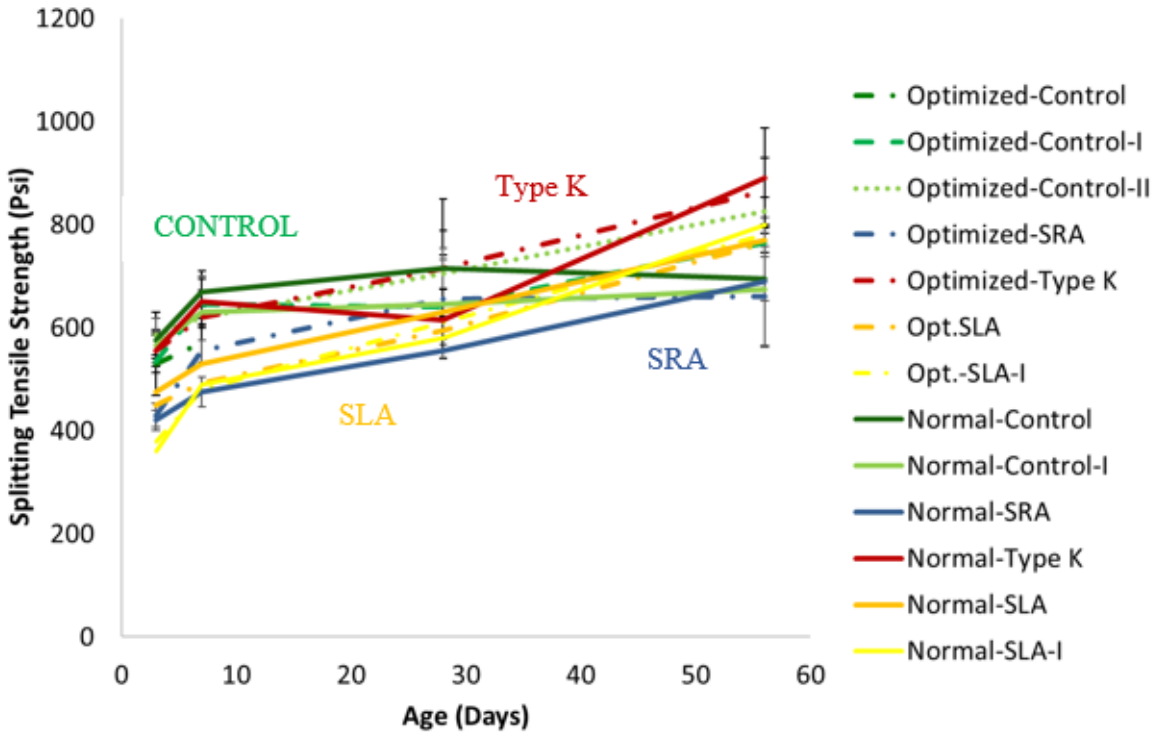

Figure 6.4 Splitting tension strength change over time for the different mixtures.

Concrete cracks when applied stress is greater than tensile strength. Since concrete weak in tension, our aim is to find out that mix design which can have highest tensile strength from early

age. Here, type K concrete shows highest amount of splitting tensile strength, then followed by control samples then SRA and SLA. It is because of bad machine performance, its load rate is not constant. In addition to that, the type of wood bearing initially were not good. Those woods were not good at transferring load. Later, as I started using another type of denser wood, I got consistent result as you can see SLA samples.

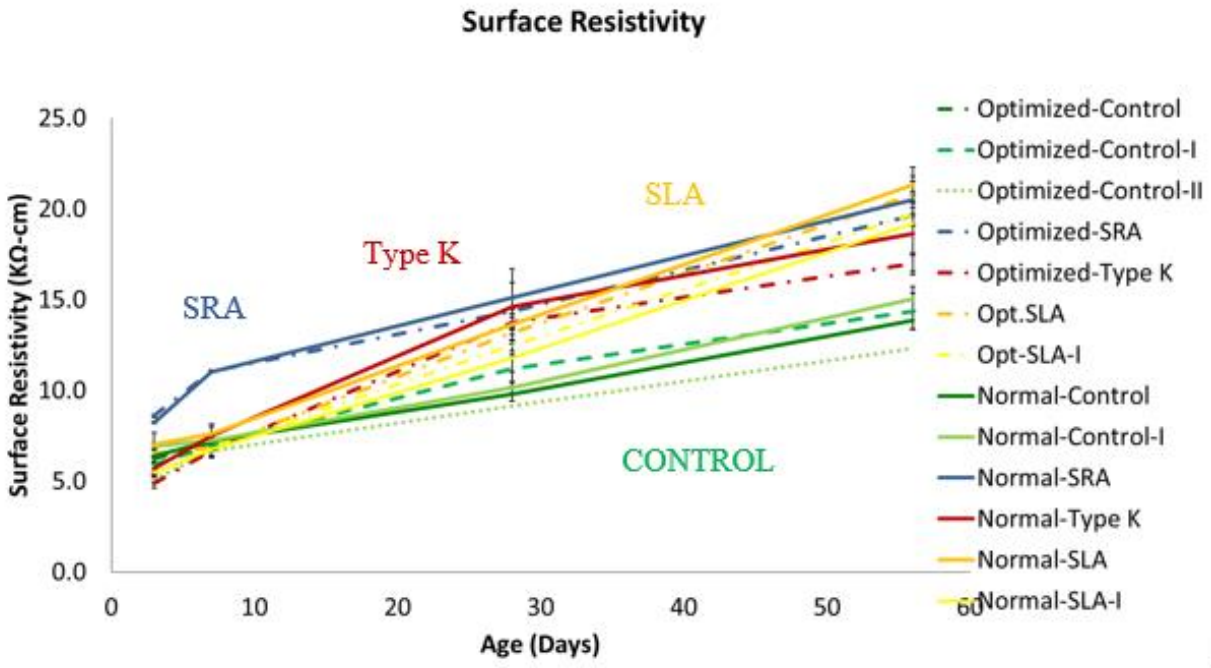

Figure 6.5 Surface resistivity change over time for the different mixtures.

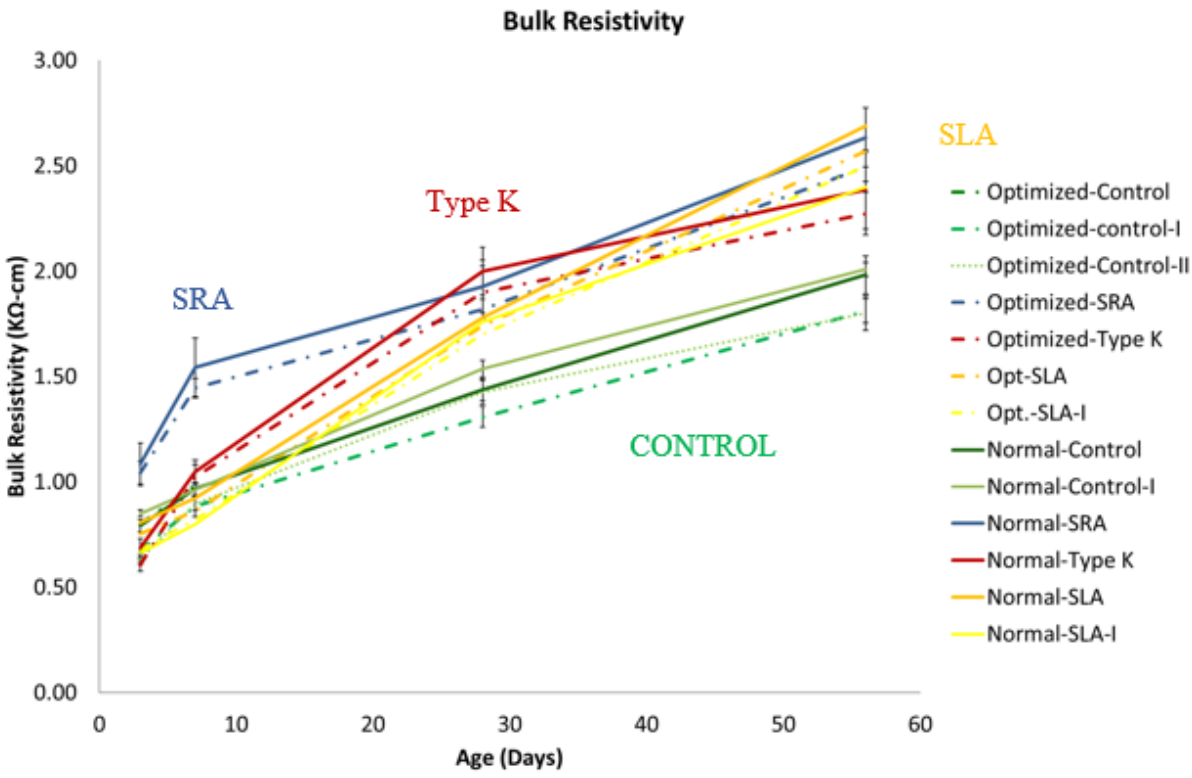

Figure 6.6 Bulk resistivity change over time for the different mixtures.

The interconnection of pores in the concrete is the reason for permeability and resistivity gives some idea regarding the conductivity of the concrete as electrical resistivity is the resistance of concrete to withstand the conductivity of ions when concrete is subjected to the electrical field.

As in other tests, optimized and non-optimized graded concrete has similar resistivity values. These are not significantly different though optimized shows lesser resistivity than non-optimized concrete.

Initially, both bulk and surface resistivity of control, type K and SLA samples have almost same resistivity values but later, the slope of graph has changed. The change in the graph indicates change in the reaction rate of each concrete. Later control samples show less resistivity, SLA samples are showing increased resistivity with age while type K sample shows large increment initially then mild increment in later stage. Increment in resistivity in Type K concrete is expected

due dense concrete formation **[12]** which contradicts with the finding of **[36]**. Out of all, SRA sample has higher resistivity than other does. It can be just due to the changes in ion conductivity rather than actual reduction in the permeability. SLA can be expected to have reduced permeability once concrete is matured. However, control samples are more conductive than any other does.

As per AASHTO TP 95, those concrete, which has surface resistivity greater than 12, allows moderate ions penetration and if it is more than 21, then it allows low ions penetration. Thus, based on this, Type K, SRA, and SLA has moderate ion penetrability while control has high ion penetrability.

Further Discussion:

Relationship among compressive strength, strain and modulus of elasticity

In order to find out predictive performance of each mixture, I have considered axial shrinkage, compressive strength, static modulus, and splitting tensile strength. I have find out percentage change in those parameters as compared to control samples. I have analyzed properties of each mixes for 3, 7, 28 and 56 days. In order to be effective concrete mixture, we need to have less shrinkage, less elastic modulus, and high splitting tensile strength. Following are the tables for illustration:

Table 4.1 showing comparison of all the mixtures

Day	3											
Mixture	Axial Shrikage			Compressive Strength			Static Modulus			Splitting Tensile Strength		
	Average	SD	Comparision	Average	SD	Comparision	Average	SD	Comparision	Average	SD	Comparision
Optimized												
Control	30	33	N/A	4260	2.5	N/A	3900	6.6	N/A	550	0.4	N/A
SRA	40	N/A	33.3	3090	N/A	-27.5	3575	N/A	-8.3	430	N/A	-21.8
Type K	435	95	1350.0	4485	10	5.3	3585	9.6	-8.1	555	10	0.9
SLA	25	45	-16.7	4315	0.8	1.3	3425	3.2	-12.2	415	0.8	-24.5
Normal												
Control	55	27	N/A	4630	4.6	N/A	3900	1	N/A	570	0.8	N/A
SRA	40	N/A	-27.3	2935	N/A	-36.6	3415	N/A	-12.4	420	N/A	-26.3
Type K	70	N/A	27.3	4740	N/A	2.4	3900	N/A	0.0	555	N/A	-2.6
SLA	30	33	-45.5	4000	4.8	-13.6	3270	0.3	-16.2	470	22.9	-17.5

Day	7											
Mixture	Axial Shrikage			Compressive Strength			Static Modulus			Splitting Tensile Strength		
	Average	SD	Comparision	Average	SD	Comparision	Average	SD	Comparision	Average	SD	Comparision
Optimized												
Control	30	28	N/A	5700	6.1	N/A	4880	2.3	N/A	610	6.8	N/A
SRA	40	N/A	33.3	4600	N/A	-19.3	3860	N/A	-20.9	555	N/A	-9.0
Type K	460	94	1433.3	5850	7.8	2.6	4145	N/A	-15.1	620	N/A	1.6
SLA	25	44	-16.7	5480	5.3	-3.9	3870	3	-20.7	530	9.9	-13.1
Normal												
Control	55	28	N/A	5925	2.7	N/A	4270	5.6	N/A	670	1.9	N/A
SRA	40	N/A	-27.3	4150	N/A	-30.0	3550	N/A	-16.9	475	N/A	-29.1
Type K	80	N/A	62.5	5850	N/A	-1.3	4065	N/A	-4.8	650	N/A	-3.0
SLA	50	6.8	-6.3	5430	3.2	-8.4	3557	2.3	-16.7	540	9.2	-19.4

Day	28											
Mixture	Axial Shrikage			Compressive Strength			Static Modulus			Splitting Tensile Strength		
	Average	SD	Comparision	Average	SD	Comparision	Average	SD	Comparision	Average	SD	Comparision
Optimized												
Control	240	6.5	N/A	6980	2	N/A	4570	1.6	N/A	670	4.9	N/A
SRA	50	N/A	-79.2	5690	N/A	-18.5	4355	N/A	-4.7	655	N/A	-2.2
Type K	IC	N/A	#VALUE!	7660	9	9.7	4600	N/A	0.7	715	N/A	6.7
SLA	250	4.2	4.2	7260	0.7	4.0	4280	0.6	-6.3	650	6.5	-3.0
Normal												
Control	195	0.1	N/A	7450	0.4	N/A	4560	1.1	N/A	680	5.1	N/A
SRA	50	N/A	-74.4	5445	N/A	-26.9	3925	N/A	-13.9	690	N/A	1.5
Type K	207	60.8	6.2	7745	N/A	4.0	4710	N/A	3.3	865	N/A	27.2
SLA	265	7.2	35.9	6610	0.3	-11.3	4160	0.6	-8.8	640	9.4	-5.9

Day	56											
Mixture	Axial Shrikage			Compressive Strength			Static Modulus			Splitting Tensile Strength		
	Average	SD	Comparision	Average	SD	Comparision	Average	SD	Comparision	Average	SD	Comparision
Optimized												
Control	310	4	N/A	7975	3.6	N/A	4880	2.3	N/A	795	3.8	N/A
SRA	90	N/A	-71.0	6530	N/A	-18.1	4235	N/A	-13.2	660	N/A	-17.0
Type K	IC	N/A	#VALUE!	8210	N/A	2.9	4905	N/A	0.5	865	N/A	8.8
SLA	295	2	-4.8	7930	1	-0.6	4395	1.7	-9.9	735	6.1	-7.5
Normal												
Control	250	3.2	N/A	8435	2.4	N/A	4910	1.9	N/A	685	1.5	N/A
SRA	93	N/A	-62.8	6180	N/A	-26.7	4365	N/A	-11.1	690	N/A	0.7
Type K	265	N/A	6.0	8590	N/A	1.8	4930	N/A	0.4	890	N/A	29.9
SLA	320	6.7	28.0	7230	1.6	-14.3	4400	1.6	-10.4	760	7.9	10.9

(In above tables, N/A means not applicable and IC means incomparable)

From the above table, SRA reduced the maximum amount of shrinkage – optimized SRA reduced shrinkage up to 79% and normal SRA up to 75% than their respective control sample at the age of day 28. Before and after day 28 the rate of shrinkage reduction is less for both the samples. Talking about other properties, compressive strength has gone down up to 37% and 27% for normal SRA and optimized SRA respectively than their respective control sample at the age of day 3. Similarly, elastic modulus had decreased up to 27 % for normal SRA at day 28 and day 56 while optimized SRA had maximum 21% less than their respective optimized control at day 7, and normal SRA had lowest splitting tensile strength up to 29% less than normal control at day 7.

Type sample showed similar expansion and shrinkage as their control samples except repeated optimized type K that showed highest expansion and lowest shrinkage as shown in figure 3.2. Optimized type K increased compressive strength up to 10% than optimized control at age of day 3 and day 28 while normal type K had slightly higher compressive strength but not that significant. Similarly, optimized type K reduced elastic modulus up to 15% than optimized control while normal type reduced elastic modulus but not that significant as optimized type K. In addition, normal type K reduced splitting tensile strength up to 30% than normal control while optimized type K had less difference in splitting tensile strength with optimized control.

Normal type K showed maximum shrinkage up to 36% higher than normal control at the age of day 28 though there is not much difference in shrinkage between optimized SLA and normal SLA. Likewise, normal SLA reduced compressive strength by 14%, static modulus by 17% and splitting tensile strength by 18%. Whereas optimized SLA does have that, much difference in compressive strength as compared with optimized control, but it reduced static modulus by 21% and splitting tensile strength by 25%.

Based on the above analysis, SRA samples worked out to be the most efficient then followed by SLA and control and then type K. Both the SRA had least amount of shrinkage from the beginning. In addition, SRA decreased modulus by large amount continuously from the beginning. Optimized SLA had almost similar shrinkage as that of optimized control and always had less elastic modulus from the beginning. However, SLA had low splitting tensile strength as compared to control as well as other samples. Repeated Type K had high expansion and lowest shrinkage, while, other two mixtures showed similar expansion as control. Good thing about type K is that this is the only mixture, which has higher splitting tensile strength than control. None of other mixtures had higher splitting tensile strength than control. Type K sample showed very variable result.

Stress Demand Vs Stress Capacity

In order to predict the performance of each concrete mix design, axial strains were taken from figure 3.1. The initially day 3 and day 7 expansion were multiplied with static modulus of same mix at day 3 and day 7 to calculate stress demand. While, for day 28 and day 56, change in shrinkages were calculated as $\epsilon_{28} - \epsilon_7$ and $\epsilon_{56} - \epsilon_7$. Here change in strain were calculated since initial expansion negates some amount of shrinkage.

Now, stress demand is calculated from following formula:

$F_t = 7.5*\sqrt{f_c'}$, Where f_c' = compressive strength, obtained from figure 4.1

Hence, following are sample graphs plotted between stress demand Vs stress capacity:

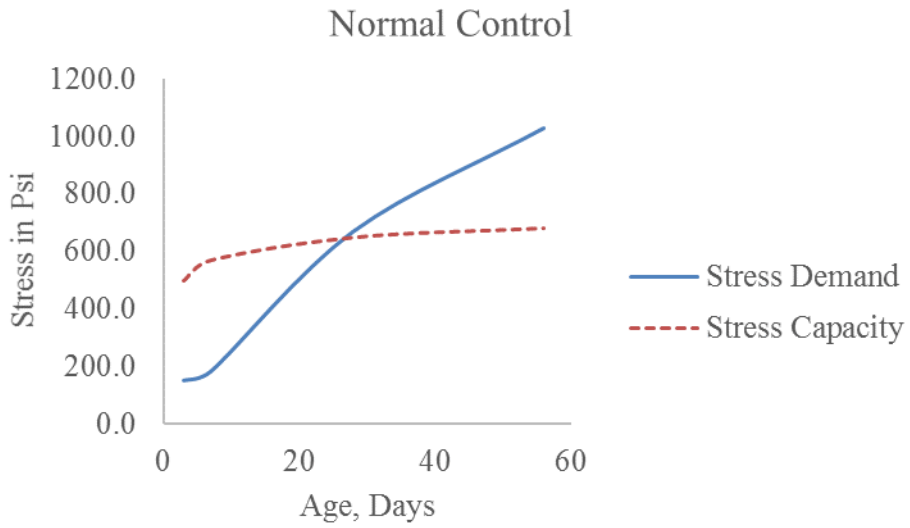

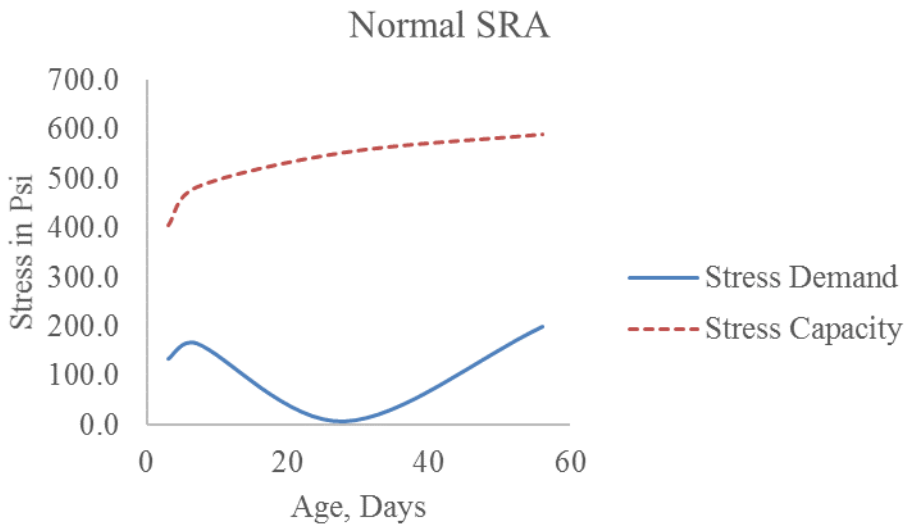

In above graphs, mostly stress demand and stress capacity lines cross each other at around 20 day. Only in case of type K mixture, these two lines cross each other at more than 20 days. Whereas in case of SRA mixture these two lines never cross each other at all. Ideally, these two lines should not cross each other unless there is crack. Since, we have not considered creep or the restraint of a

structure, the stress demand and stress capacity lines cross each other. While, this may not be the case in the field it provides a useful method to compare the results to one another.

Hence, this is the summary table for drying days to before cracking:

Table 4.2 showing comparison of drying day before cracking

Mixture	Control		SRA		Type K		SLA	
	Optimized	Normal	Optimized	Normal	Optimized	Normal	Optimized	Normal
Day	20	23	∞	∞	33	38	20	20
SD	0.7	4	N/A	N/A	5	N/A	0.7	0.7

Based on this table, it takes infinity number of days for SRA concrete to have cracking. After that, type K concrete takes higher number days to crack, followed by control and SLA concrete.

CHAPTER V

CONCLUSION AND RECOMMENDATION

Out of all eight-mixture designs, there is no significant difference between optimized and non-optimized graded concrete in terms of shrinkage as well as other mechanical properties. Thus, it can be recommended to use optimized graded concrete since it uses less amount of paste, which is economical. Next, SRA has shown very good performance; showed less shrinkage and less modulus. Therefore, if we can find out proper air entraining practices then this can be a useful concrete mixture to reduce cracking and provide long term durability.

While SLA had less static modulus than control and type K concrete, which is desirable property for bridge deck cracking. With same amount of strain and low amount of static modulus, concrete can have less amount of stress in it. Lesser the stress in concrete less would be the possibility of cracking. It is recommended to try further investigate SLA and SRA by constructing a full scale bridge deck to investigate the performance of the materials.

REFERENCES

1. Torben, C.H. and H.M. Alan, *Influence of Size and Shape of Member on the Shrinkage and Creep of Concrete.* Journal Proceedings. 63(2).
2. Bremner, T.W. and T.A. Holm, *Elastic Compatibility and the Behavior of Concrete.* Journal Proceedings. 83(2).
3. Institute, A.C., *ACI 305. 1M-14 Specification for Hot Weather Concreting*. 2014: American Concrete Institute.
4. Mindess, S. and J.F. Young, *Concrete*. 1981: Prentice-Hall.
5. Folliard, K.J. and N.S. Berke, *Properties of high-performance concrete containing shrinkage-reducing admixture.* Cement and Concrete Research, 1997. 27(9): p. 1357-1364.
6. Balogh, A., *Concrete Construction Article PDF- New Admixture Combats Concrete Shrinkage.* Concrete Construction-The Aberdeen Group, 1996(#C960546).
7. Rajabipour, F., G. Sant, and J. Weiss, *Interactions between shrinkage reducing admixtures (SRA) and cement paste's pore solution.* Cement and Concrete Research, 2008. 38(5): p. 606-615.
8. Evans, D.F., *The colloidal domain : where physics, chemistry, biology, and technology meet*, ed. H.k. Wennerström. 1994, New York, NY: New York, NY : VCH Publishers.
9. Zana, R., *Introduction to Surfactants and Surfactant Self-Assemblies*, in *Dynamics of Surfactant Self-Assemblies*. 2005, CRC Press. p. 1-35.
10. Frederick R. Keith, W.W.W. and A.H. Jerry, *A Peach Of A Pavement Using Shrinkage-Compensating Concrete.* Concrete International. 18(5).
11. Rubin, E., *Crack-Free Bridge Decks Brochure* Concrete Construction Jan 2006.

12. Paul W. Grunner, G.A.P., *Type K Shrinkage Compensating Cement in Bridge Deck Concrete.* ACI Concrete International

Oct. 1993.

13. Weiss, J., *Internal Curing - CP Road Map.* Federal Highway Administration, Dec. 2015.

14. Lopez, M., L.F. Kahn, and K.E. Kurtis, *Characterization of elastic and time-dependent deformations in high performance lightweight concrete by image analysis.* Cement and Concrete Research, 2009. 39(7): p. 610-619.

15. Shin, K., et al., *The Role of Internal Curing as a Method to Improve Durability.* S. Kim, & K. Ann (Ed.), Handbook of Concrete Durability, 2010: p. 379-428.

16. *Standard Specification for Concrete Aggregates*. 2016, ASTM International.

17. *Standard Specification for Expansive Hydraulic Cement*. 2012, ASTM International.

18. *Standard Specification for Portland Cement*. 2017, ASTM International.

19. *Standard Specification for Coal Fly Ash and Raw or Calcined Natural Pozzolan for Use in Concrete*. 2015, ASTM International.

20. *Standard Test Method for Slump of Hydraulic-Cement Concrete*. 2015, ASTM International.

21. *Standard Test Method for Density (Unit Weight), Yield, and Air Content (Gravimetric) of Concrete*. 2017, ASTM International.

22. *Standard Test Method for Air Content of Freshly Mixed Concrete by the Pressure Method*. 2017, ASTM International.

23. *Standard Test Method for Length Change of Hardened Hydraulic-Cement Mortar and Concrete*. 2014, ASTM International.

24. Hajibabaee, A. and M.T. Ley, *The impact of wet curing on curling in concrete caused by drying shrinkage.* Materials and Structures, 2015. 49(5): p. 1629-1639.

25. *Standard Test Method for Fundamental Transverse, Longitudinal, and<brk/> Torsional Resonant Frequencies of Concrete Specimens*. 2014, ASTM International.

26. *Surface Resistivity Test - AASHTO TP 95.* Mar 2013.

27. *Standard Test Method for Compressive Strength of Cylindrical Concrete Specimens*. 2017, ASTM International.

28. Testing, A.S.f., et al., *ASTM C496: Standard Test Method for Splitting Tensile Strength of Cylindrical Concrete Specimens*. 2011: ASTM International.

29. *Standard Test Method for Static Modulus of Elasticity and Poisson’s Ratio of Concrete in Compression*. 2014, ASTM International.

30. board, T.R., *Control of Cracking in Concrete - State of Art.* Transportation Research Circular No. E-C 107, Oct. 2006.

31. Hamed Layssi, P.G., Aali R. Alizadeh, Mustafa Salehi, *Electrical Resistivity of Concrete.* Concrete International 37 (5) : 41-46 May 2015.

32. JoAnn Browning, D.D.D.R. and P. Benjamin, *Lightweight Aggregate as Internal Curing Agent to Limit Concrete Shrinkage.* Materials Journal. 108(6).

33. Hobbs, D.W., *Influence of Aggregate Restraint on the Shrinkage of Concrete.* Journal Proceedings. 71(9).

34. Weiss, W.J., *Prediction of Early-age Shrinkage Cracking in Concrete Elements /by William Jason Weiss*. 1999: UMI Dissertation Services.

35. Neville, A.M., *Properties of concrete*. 1981: Pitman Pub.

36. Sedat Gulen, J.J.S., *Expansion Centre in Bridge Decks.* Final Report for the Division of Research and Training of the Indiana Department of Highways, March 1984.

37. Lu, X., et al., *Evaluation of dynamic modulus of elasticity of concrete using impact-echo method.* Construction and Building Materials, 2013. 47: p. 231-239.

VITA

Bijaya Laxmi Rai

Candidate for the Degree of

Master of Science

Thesis: MIXTURE DESIGNS TO MITIGATE BRIDGE DECK CRACKING DUE TO SHRINKAGE

Major Field: Civil Engineering

Biographical:

Education:

Completed the requirements for the Master of Science in Civil Engineering at Oklahoma State University, Stillwater, Oklahoma in July, 2017.

Completed the requirements for the Bachelor of Science in Civil Engineering at Purwanchal University, Biratnagar, Nepal in Nov 2013.

Experience:

- Worked on development of different mixture designs to mitigate bridge deck cracking due to shrinkage as a Graduate Research Assistant in Civil Engineering Laboratory of Oklahoma State University, 2015-2017

- Worked as Assistant Design and Planning Engineer at Sanjen (Upper) Hydroelectric Project, Rasuwa-Kathmandu, Nepal, 2013-2015

- Worked as Article Contributor for Spaces Magazine, Kathmandu-Nepal, 2014-2015

- Worked as Secondary level Teacher in Geetanjali English School, Kathmandu-Nepal, 2008-2009

Professional Memberships:

- Engineer in Training, NCEES Board since 2017
- Member of American Institute of Steel Construction since 2016
- Member of American Concrete Institute since 2015
- Registered Civil Engineer of Nepal Engineering Council since 2014